

**The *TORNADO2* gene of *Arabidopsis thaliana* affects
cellular decisions in the shoot apical meristem.**

Inaugural-Dissertation

Zur Erlangung des Doktorgrades der Mathematisch-
Naturwissenschaftlichen Fakultät der Universität zu Köln

vorgelegt von

Wei-Hsin, Chiu

aus Kaohsiung, Taiwan

Köln 2006

Gutachter: Prof. Dr. Wolfgang Werr
Prof. Dr. U. I. Flügge

Tag der mündlichen Prüfung: 5 Juli 2006

INDEX

1. INTRODUCTION.....	1
1.1 The shoot apical meristem (SAM) of <i>Arabidopsis</i>	1
1.1.1 The properties and the organization of the SAM.....	1
1.1.2 The homeostasis of the stem cell niche in the SAM.....	2
1.2 The <i>SHOOT MERISTEMLESS (STM)</i> gene.....	3
1.2.1 <i>STM</i> functions in initiating and maintaining the SAM.....	3
1.2.2 <i>STM</i> maintains the indeterminate state of cells in meristems and is downregulated in lateral organ primordia.....	5
1.2.3 <i>STM</i> and its interacting partners	6
1.3 Plant hormone auxin.....	7
1.4 Tetraspanin proteins.....	8
1.4.1 Tetraspanin proteins are implicated in divergent biological processes.....	9
1.4.2 Tetraspanins structural properties and the TEM.....	10
1.5 The aim of this project.....	11
2. MATERIALS AND METHODS.....	12
2.1 Plant materials and growth conditions.....	12
2.2 Chemicals and enzymes.....	12
2.3 Buffers, solutions and media.....	13
2.4 Bacteria and vectors.....	13
2.4.1 Bacteria strains.....	13
2.4.2 Vectors.....	13
2.5 Oligonucleotides.....	13
2.6 Genetic mapping.....	16
2.7 Molecular biology methods.....	16
2.7.1 Standard molecular biology methods.....	16
2.7.2 Transformation of bacteria (<i>E. coli</i>)	16
2.7.3 Preparation of plasmid DNA	17
2.7.4 The extraction of the genomic DNA from <i>Arabidopsis thaliana</i>	17

2.7.5 The extraction of total RNA from <i>Arabidopsis thaliana</i> and the synthesis of <i>cDNA</i>	17
2.7.6 Polymerase chain reaction (PCR)	18
2.7.7 Real-time PCR.....	18
2.7.7.1 The principle of real-time PCR.....	18
2.7.7.2 Preparation and manipulation of real-time PCR reactions.....	20
2.7.8 Non-radioactive RNA <i>in situ</i> hybridization.....	21
2.8 Histology.....	21
2.8.1 Fixation, embedment and sections of the plant tissue.....	21
2.8.1.1 Preparation of the fixative.....	21
2.8.1.2 Fixation of samples.....	22
2.8.1.3 Embedment of samples.....	22
2.8.1.4 Sections.....	22
2.8.2 Microscopic technique.....	23
2.8.3 GUS staining.....	23
2.9 Computer analysis.....	23
3. RESULTS.....	24
3.1 Identification of the mutant line 3010.....	24
3.2 The mutant phenotype of the line 3010.....	26
3.2.1 The morphology of the mutant.....	26
3.2.2 The plastochron index and the flowering time of the mutant.....	28
3.3 Genetic mapping and allelism test.....	29
3.4 <i>TRN2</i> encodes a tetraspanin-like protein.....	32
3.5 RNA <i>in situ</i> hybridization of <i>TRN2</i> and other meristem-related genes.....	34
3.5.1 The <i>TRN2</i> expression pattern.....	34
3.5.2 <i>STM</i> expression pattern in <i>trn2</i> mutants.....	36
3.5.3 <i>WUS</i> and <i>CLV3</i> expression patterns in <i>trn2</i> mutants.....	37
3.5.4 <i>LFY</i> expression in <i>trn2</i> mutants.....	39
3.6 Real-time RT-PCR experiments.....	40
3.7 Genetic interactions between <i>trn2</i> and other meristem-related genes.....	41
3.7.1 Genetic interactions between <i>trn2</i> and <i>stm</i>	42
3.7.1.1 <i>stm-5</i> and <i>stm-1</i> alleles.....	42

3.7.1.2	Identification of double mutants for both <i>trn2</i> and <i>stm</i>	42
3.7.1.3	Phenotypic analyses of <i>trn2 stm</i> double mutants.....	44
3.7.2	<i>trn2</i> and <i>wus</i>	46
3.7.2.1	The <i>wus-1</i> allele.....	46
3.7.2.2	Genetic interactions between <i>wus-1</i> and <i>trn2₃₀₁₀</i>	46
3.7.3	<i>trn2</i> and <i>clv3</i>	48
3.7.3.1	The <i>clv3-2</i> mutant.....	48
3.7.3.2	Genetic interactions between <i>clv3-2</i> and <i>trn2₃₀₁₀</i>	49
4.	DISCUSSION.....	51
4.1	The <i>TRN2</i> gene encodes a tetraspanin-like protein.....	51
4.2	<i>TRN2</i> may contribute to another pathway rather than to <i>STM</i> pathway directly.....	52
4.3	<i>trn2</i> mutation affects cell fate decisions in the SAM.....	53
4.4	<i>TRN2</i> affects auxin distribution and vasculature patterning in leaves.....	55
4.5	<i>trn2</i> mutation compensates meristem defects of <i>stm</i> and <i>wus</i> mutants.....	56
4.6	Genetic interactions between <i>trn2</i> and <i>clv3</i>	57
4.7	<i>TRN2</i> contributes to maintain a normal meristem function.....	58
5.	SUMMARY.....	61
6.	ZUSAMMENFASSUNG.....	62
7.	BIBLIOGRAPHY.....	64
	<i>ERKLÄRUNG</i>.....	73
	<i>ACKNOWLEDGEMENTS</i>.....	74
	<i>LEBENS LAUF</i>	75

1. INTRODUCTION

1.1 The shoot apical meristem (SAM) of *Arabidopsis thaliana*

1.1.1 The organization and the properties the SAM

The aerial structures of higher plants are dynamically generated throughout the life cycle by the activity of pluripotent stem cells that are located at the growing shoot tip, the SAM. During the vegetative stage in *Arabidopsis*, plants have an indeterminate SAM that generates leaves repetitively in a stereotypical pattern known as phyllotaxy, and can, theoretically, grow indefinitely. When the floral transition process begins, the shape of the SAM changes (both in width and height) and it generates floral meristems and a bolting inflorescence shoot decorated with cauline leaves. Floral meristems, in contrast with SAMs, are determinate—they will be terminated after the formation of flowers and do not grow indefinitely. The SAM of *Arabidopsis thaliana*, and most other dicotyledonous plants, is organized into distinct layers and zones. The first level of SAM organization is the stratification of the cells into tunica and corpus layers. The tunica consists of the L1 layer (the outermost layer that is just one cell thick) and the L2 layer (also one cell thick and lies beneath L1). In both L1 and L2, cell divisions are anticlinal, that is, the new cell walls are formed perpendicular to the surface of the meristem, thus maintaining the organization of these layers. The L1 layer gives rise to the epidermis and the L2 layer forms the subepidermal layer and the gametes. The corpus, or the L3 layer, which lies beneath the tunica, has variable patterns of division and it transitions into the stem at the meristem base. The SAM is further organized into three functionally distinct zones. The peripheral zone (PZ) and the rib zone (RZ) contain cells that will become incorporated into lateral organ primordia and the stem core, respectively. The central zone (CZ), which is surrounded by the PZ and characterized by a lower mitotic activity, constitutes the self-renewing pluripotent stem-cell reservoir. Cell divisions in the CZ cause displacement of daughter cells outward into the PZ. Once the progeny of the stem cells have left the CZ, they are recruited for organogenesis and eventually differentiate. Cells in the CZ also divide downward into the RZ, which contributes to the meristem pith. The CZ concomitantly replenishes itself through these cell divisions. In this way, the SAM mediates plant growth and sustains itself as a stable structure, in spite of the constant flow of cells passing through it (for reviews, see: Brand *et al.*, 2001; Carles and Fletcher, 2003; Doerner, 2003).

1.1.2 Maintenance of the homeostasis of the stem cell niche in the SAM

Genetic analyses in *Arabidopsis thaliana* have identified a number of genes involved in meristem function. SAM maintenance is disrupted by a loss-of-function mutation in the *WUSCHEL* (*WUS*) locus. The *WUS* gene encodes a homeodomain protein that is expressed in a small group of cells located in the meristem center underneath the presumed position of the stem cells (Mayer *et al.*, 1998). *wus* mutants do form an embryonic SAM. However, shoot meristems initiate repetitively in these mutants, but prematurely terminate in aberrant flat structures during the vegetative phase. In addition, *wus* inflorescence meristems produce fewer flowers compared with wild-type plants and those flowers usually terminate prematurely in a single stamen (Laux *et al.*, 1996). It has been proposed that this defective meristem phenotype results from a loss of stem cells in the CZ that, in turn, cannot sustain the meristem (Laux *et al.*, 1996). In contrast with *wus*, which causes premature meristems, loss-of-function mutations at the *clavata* loci (*clv1*, *clv2* and *clv3*) lead to enlarged meristem phenotypes. *clv* mutants not only have enlarged meristems but also have an increased number of organ primordia with an apparent altered phyllotaxy and supernumerary carpels at the floral center (Clark *et al.*, 1993). Similar phenotypes of all three *clv* mutants suggest that wild-type *CLV* genes function in the same genetic pathway. The *CLV1* gene encodes a receptor-like kinase that contains an extracellular domain composed of 21 tandem leucine-rich repeats (LRR) and a predicted cytoplasmic domain that acts as a serine kinase, suggesting a role in signal transduction. *CLV1* transcripts are detected in a patch of cells across the center of the meristem in the L2 layer and predominately in the L3 layer (Clark *et al.*, 1997). The *CLV2* gene encodes a receptor-like protein with LRRs; however, its cytoplasmic tail is short and lacks a kinase domain (Jeong *et al.*, 1999). *CLV2* transcripts have been detected in shoots and flowers based on RNA gel blot analysis (Jeong *et al.*, 1999), but its precise domain of expression in meristems has yet to be determined. The *CLV2* protein is required for the accumulation of *CLV1* and its assembly into protein complexes, indicating that *CLV2* may form a heterodimer with *CLV1* to transduce extracellular signals (Jeong *et al.*, 1999). The *CLV3* gene encodes a protein of 96 amino acids and an 18-amino acid long, NH₂-terminal hydrophobic region in this protein may function as a signal peptide to direct the protein into the secretory pathway (Fletcher *et al.*, 1999). *CLV3* transcripts are detected in the upper two layers of the CZ and in a few underlying L3 cells, and its expression domain is proposed to be a molecular marker for stem cells (Fletcher *et al.*, 1999). Based on analysis of expression domains, *CLV3* transcripts are largely found beneath the

INTRODUCTION

CLV1 expression domain, suggesting that *CLV1*-expressing cells may communicate with *CLV3*-expressing cells through a signal transduction pathway. Consistent with this, it has been reported that *CLV3* is localized to the extracellular space, and that this apoplastic localization is required for *CLV3* to activate a hypothesized CLAVATA signaling pathway (Rojo *et al.*, 2002). Furthermore, it has also been shown that *CLV3* signaling occurs through a *CLV1/CLV2* receptor complex (Brand *et al.*, 2000).

In an enlarged meristem of a *clv3* mutant, the *WUS* expression domain is expanded, and ectopic expression of *WUS* is observed in *clv3* embryos and floral meristems (Schoof *et al.*, 2000). On the other hand, in an arrested meristem (reminiscent of the *wus* phenotype) of a plant overexpressing *CLV3*, *WUS* transcripts were not detectable by RNA *in situ* hybridization (Brand *et al.*, 2000). These results indicate that *CLV* signaling negatively regulates *WUS* expression. The *wus clv* double mutants have a phenotype indistinguishable from *wus* single mutants during vegetative development, suggesting that these genes act in a common pathway and *WUS* is required for the *clv* phenotype (Laux *et al.*, 1996; Schoof *et al.*, 2000). *WUS* expression under the control of the *CLV1* promoter leads to expansion of the meristem and the expression of *CLV3*, suggesting that *CLV3* is controlled by *WUS* (Schoof *et al.* 2000). These observations lead to the development of a model for homeostasis within the stem cell niche. *WUS* and *CLV* comprise a feedback loop, such that *WUS* acts cell-nonautonomously to promote stem-cell identity and *CLV3* expression through an as yet unknown signal, while the *CLV3* polypeptide, in turn, acts as a ligand to bind to the *CLV1/CLV2* receptor complex thus activating the signaling pathway that represses *WUS* expression. Within this loop, stem cell identity is established and maintained by the signal from the organizing center (OC) where *WUS* is expressed, and the OC size is then limited by the signal given back from stem cells where *CLV3* is expressed.

1.2 The *SHOOT MERISTEMLESS (STM)* gene

1.2.1 *STM* functions in initiating and maintaining the SAM

In addition to the stem-cell homeostasis in the CZ described above, another important question is how the entire SAM is initiated and maintained. In maize, the homeobox gene *KNOTTED1 (KNI)* has proved to be a useful molecular marker for SAM (Smith *et al.*, 1995). The onset of *KNI* expression during embryogenesis coincides with the first histological features that

INTRODUCTION

characterize SAM formation in maize (Smith *et al.*, 1995) and expression persists in the vegetative SAM, axillary meristems, terminal and lateral inflorescence meristems (tassel and ear, respectively), and in both male and female floral meristems (Smith *et al.*, 1995). Loss-of-function mutations in *kn1* gene are defective in shoot-meristem maintenance (Kerstetter *et al.*, 1997). In *Arabidopsis*, the *KNOTTED*-like homeobox (*KNOX*) genes, which are defined by homology to the maize *KN1* gene, comprise eight members. The best characterized of these is the *STM* gene. Like other *KNOX* genes, the *STM* gene encodes a homeodomain protein belonging to a superfamily — the three amino acid extension (TALE) family. However, in addition to the TALE homeodomain (TALE-HD), the *STM* protein (and other *KNOX* proteins) has a conserved ELK domain and a MEINOX (Cole *et al.*, 2006) domain that may function in protein-protein interactions. *STM* expression is first apparent in early to mid-globular stage embryos, where it is found in one or two cells (Long *et al.*, 1996). By the early heart stage of embryogenesis, expression is found in a continuous band between the presumptive cotyledons and by the torpedo and walking-stick stages of embryogenesis, the expression is confined to the tip of the embryo, where the primary meristem is located (Long *et al.*, 1998).

A loss-of-function allele, *stm-1*, was identified and its seedlings were shown to lack a SAM but were otherwise healthy and viable, suggesting that *STM* functions specifically in the establishment of the SAM (Barton and Poethig, 1993). Furthermore, the configuration of cells in the apical position of *stm-1* end-stage embryos and young seedlings was similar to that seen in torpedo stage embryos, revealing that the *stm-1* completely blocks the initiation of the SAM at, or just after, the torpedo stage of embryogenesis (Barton and Poethig, 1993). Tissue cultures from *stm-1* seedlings grown in medium that promotes shoot regeneration only produced abnormal leaves or shoots and gave rise to fewer such structures than wild-type tissue (Barton and Poethig 1993). *stm-1* mutation thus affects the initiation of the SAM in culture (Barton and Poethig 1993). These results indicate that *STM* locus is required for SAM initiation both embryonically and postembryonically (Barton and Poethig 1993). Taken together, these results indicate that *STM* is required for the establishment of a functional primary SAM.

STM expression persists into the seedling and adult plant, where it is present in all SAMs: vegetative, axillary, inflorescent and floral (Long *et al.*, 1996). Analysis of the defects in an allelic series of *stm* mutants showed that all postembryonic structures can be formed in all alleles, however, *stm* mutation often leads to fused primordia (Endrizzi *et al.*, 1996). *stm* floral

meristems also displayed similar defects and terminated prematurely in central stamens (Endrizzi *et al.*, 1996), which are reminiscent of *wus* mutants, thus implying loss of the meristem activity. The persistence of *STM* expression and *stm* phenotypes suggest that *STM* activity is required for SAM maintenance, as well as initiation.

1.2.2 *STM* maintains the indeterminate state of cells in meristems and is downregulated in lateral organ primordia

STM is expressed throughout the shoot tip, yet there are regions that lack expression. These *STM*-negative regions, which coincide with early steps (P0) in the development of lateral organ primordia, indicate that *STM* is downregulated while organ primordia are initiated (Long *et al.*, 2000). Thus, *STM* expression is specifically confined to indeterminate cells within shoot meristems. Furthermore, loss-of-function *stm* mutant seedlings develop cotyledons and leaves that are fused at their bases, suggesting that cells in the center of *stm* shoot meristems, which in wild-type plants remain undifferentiated, appear to become incorporated into ectopic primordia and undergo differentiation (Endrizzi *et al.*, 1996). Therefore, the indeterminate state of cells within the SAM is dependent on the *STM* gene. In addition, downregulation of *STM* in lateral organ primordia has been shown to be a critical event in organ development, as ectopic expression of *STM* disrupts normal leaf development (Chuck *et al.*, 1996; Williams, 1998). Hence, lack of *STM* expression is a useful molecular marker for lateral organ primordia.

In *Arabidopsis*, two other *KNOX* genes, *KNAT1* and *KNAT2*, have similar expression patterns to *STM* (Lincoln *et al.*, 1994; Serikawa *et al.*, 1996); both genes are expressed throughout the vegetative SAM but are specifically excluded from initiating leaf primordia and mature leaves. Based on the similarity of residues within the homeodomain of the proteins, the intron positions and the expression patterns (Hake *et al.*, 2004; Reiser *et al.*, 2000), *STM*, *KNAT1* and *KNAT2* are referred to as class I *KNOX* genes. Overexpression of *KNAT1* in transgenic *Arabidopsis* altered leaf development and caused the formation of ectopic meristems (Chuck *et al.*, 1996; Lincoln *et al.*, 1994). Thus, exclusion of class I *KNOX* gene activity from peripheral founder cells appears to be crucial in leaf cell fate acquisition.

Plants with a loss-of-function mutation in *ASSYMETRIC1* (*ASI*) or *AS2* have a phenotype similar to *KNAT1* overexpression, suggesting that *ASI* and *AS2* genes negatively regulate *KNAT1*

INTRODUCTION

expression (Byrne *et al.*, 2000; 2002). The *AS1* gene encodes a Myb domain transcription factor and its transcripts are first detectable in late globular stage, maintained in developing cotyledons, but absent in cells that subsequently form the SAM (Byrne *et al.*, 2000). Later, its transcripts are detected in leaf founder cells from the time of primordium initiation until stage P4 (Byrne *et al.*, 2000). Genetic interactions between *as1* and *stm* demonstrate that *as1* can rescue the *stm* phenotype in embryonic and vegetative meristems (Byrne *et al.*, 2000), and *AS1* expression spreads throughout the apical region in *stm* embryos (Byrne *et al.*, 2000). These results suggest that *STM* negatively regulate *AS1* expression. *as1* leaf phenotype is comparable with *as2* mutants, which have class I *KNOX* genes also miss-expressed (Ori *et al.*, 2000; Semiarti *et al.*, 2001). *AS2* is also negatively regulated by *STM* and it is likely that it interacts with *AS1* and negatively regulates other class I *KNOX* genes (Byrne *et al.*, 2002). These observations generate a model of mutual negative interactions between *MYB* and class I *KNOX* genes. In the wild-type meristem *STM* is on and it keeps *AS1* and *AS2* off. This allows the class I *KNOX* genes and other targets required for meristem function to be on. In leaf founder cells, all class I *KNOX* genes are downregulated by some unknown mechanism. In slightly older leaf primordia (P2 stage and beyond) the activity of *AS1* and *AS2* maintains *KNAT* genes repression while another yet unknown factor maintains *STM* repression (Barton, 2001; Byrne *et al.*, 2002). Together, this pathway functions to distinguish organ founder cells from meristem cells in the SAM, allowing for tightly controlled regulation of lateral organ cell fate.

1.2.3 *STM* and its interacting partners

TALE homeobox genes are found in plants, animals and fungi (Hake *et al.*, 2004; Reiser *et al.*, 2000), and the interactions between TALE-HD proteins, which have important functions in the developmental processes of both animal and fungi, have been explored (Bellaoui *et al.*, 2001). It has been shown that the *Arabidopsis* *KNOX* TALE-HD proteins interact with BELL1-like homeodomain (BLH) proteins, also TALE-HD proteins, through the N-terminal MEINOX domain (Bellaoui *et al.*, 2001; Muller *et al.*, 2001; Smith *et al.*, 2002). The *KNOX*/BLH complex mediates high affinity DNA binding *in vitro* and this interaction is selective, suggesting that *KNOX* proteins have a greater affinity for certain BLH proteins than for others (Bellaoui *et al.*, 2001; Smith *et al.*, 2002). The overlapping patterns of *BEL1* and *STM* expression within the inflorescence meristem suggest a function for the *BEL1*/*STM* complex in maintaining the indeterminate status of the inflorescence meristem (Bellaoui *et al.*, 2001). Three BLH proteins,

INTRODUCTION

ATH1, *BLH3* and *BLH9*, were identified as interacting partners of *STM* in yeast two-hybrid studies (Cole *et al.*, 2006). As a potential transcriptional factor, *STM* would be expected to be localized to the nucleus. However, fusion proteins of *STM* and GFP are cytoplasmic when they are expressed in leek, onion or *Arabidopsis* hypocotyl epidermal cells (Cole *et al.*, 2006), suggesting that the *STM* protein is not located in the nucleus by default. Conversely, bimolecular fluorescence complementation (BiFC) substantiates the nuclear localization of *STM* through heterodimerization with the previously mentioned BLH partner proteins (Cole *et al.*, 2006). *ATH1*, *BLH3* and *BLH9* are expressed in the inflorescence meristem (IFM) in discrete domains, suggesting that the IFM is divided into zones, from the center to the periphery (Cole *et al.*, 2006). Furthermore, overexpression of these *BLH* genes affected flowering time, and when combined with inducible *STM* expression of *STM-GR* (Brand *et al.*, 2002), additive phenotypes of early flowering were observed in the pre-conditioned ectopic *ATH1* or *BLH3* background, and a lobbed leaf phenotype was observed in the pre-conditioned ectopic *BLH9* background (Cole *et al.*, 2006). Taken together, these results suggest that *STM* may interact with specific BLH proteins in the center and periphery of the shoot apex to contribute to different functions.

1.3 Plant hormone auxin

The plant hormone auxin has divergent functions in various developmental processes. Auxin is actively distributed within the plant by efflux- and influx-dependent cell-to-cell movement. The direction of auxin flow was suggested to be mediated by the asymmetric cellular localization of efflux carriers, probably represented by plant-specific PIN-FORMED (PIN) proteins.

During embryogenesis, the auxin response gradient is first established basipetally and at about the 32-cell stage, is reversed to become acropetal (Friml *et al.*, 2003). Application of auxin-efflux inhibitors perturbs the polar distribution pattern of auxin during embryogenesis, suggesting that the polar distribution of auxin in embryos is mediated by auxin efflux (Friml *et al.*, 2003). The polar distribution of auxin establishes an apical-basal axis that is crucial for embryogenesis. Disruptions of the polar distribution of auxin are always accompanied by embryo defects (Friml *et al.*, 2003). Auxin transport and its polar distribution also have key functions in shoot organogenesis. During the establishment of the lateral organ primordia of shoots, auxin is transported to, and accumulated at, the primordium tip to establish an auxin gradient prior to lateral organ formation (Benková *et al.*, 2003). Treatment of the SAM with auxin-efflux

inhibitors results in a pin-like inflorescence, without any lateral organ (Benková *et al.*, 2003).

PIN proteins are membrane proteins and are known as auxin-efflux facilitators (Galweiler *et al.*, 1998). There are 8 members of PIN protein family in *Arabidopsis* (Friml, 2003; Friml *et al.*, 2003), but only 4 of them, *PIN1*, *PIN3*, *PIN4* and *PIN7*, are expressed in embryos and are implicated in auxin transport (Friml *et al.*, 2003). During embryogenesis, the initial auxin-dependent specification of the apical cell relies on the efflux activity of the PIN7 protein that is localized on the apical face of the basal cell. At approximately the 32-cell stage, auxin flux is reversed following retargeting of both PIN1 and PIN7 proteins to the basal faces of provascular and basal cells, respectively (Friml *et al.*, 2003). Multiple combinations of *pin* mutants revealed functional redundancy among PIN proteins (Friml *et al.*, 2003). The PIN efflux-carrier activity is also required during the formation of lateral organ primordia. Recent data provide evidence that auxin is transported towards founder cells of new organ primordia involving changes in the distribution of PIN proteins at the plasma membrane (Reinhardt *et al.*, 2003).

In addition to embryogenesis and organogenesis, auxin also has a central role in vascular patterning. Throughout leaf development, auxin accumulation is restricted to subepidermal cell layers (Mattsson *et al.*, 2003). Auxin is strongly accumulated at the distal tip in very early stage leaf primordia and is weakly accumulated in the incipient primary vein (Mattsson *et al.*, 2003). As leaf primordia develop, auxin accumulation disappears in the mature primary vein but becomes apparent where incipient secondary veins emerge, and then in a series in tertiary and quaternary veins, and finally completely disappears in mature vessels (Mattsson *et al.*, 2003). As the primary midvein develops acropetally, and secondary veins develops in a basipetal sequence, it has been proposed that auxin induces the formation of a vascular strand along which auxin is subsequently transported in a polar fashion (Reinhardt, 2003). Thus, auxin accumulation precedes oriented cell divisions, which produce continuous files of narrow procambial cells, and disappear at later differentiation stages.

1.4 Tetraspanin proteins

Extracellular stimuli, such as CLV3 ligands and some plant hormones, have to interact with membrane proteins to transduce signals through distinct signaling pathways. This crosstalk between cell-surface stimuli and signaling pathways needs to be regulated. In animals, the

regulation of cell-surface stimuli and signaling pathways can be modulated by tetraspanin proteins. Tetraspanins are a large family of transmembrane proteins that form ‘tetraspanin-enriched microdomains’ (TEMs) on the cell membrane and function as specific membrane docks — they cluster associated membrane proteins and interact with intracellular signaling proteins.

1.4.1 Tetraspanin proteins are implicated in divergent biological processes

To our knowledge, there are at least 33 tetraspanins in mammals, 36 in *D. melanogaster* and 20 in *C. elegans* (Hemler, 2005; Levy and Shoham, 2005; Huang, 2005). In humans and mice, CD81, which was originally identified as a target of an anti-proliferation antibody on human B cells (Oren *et al.*, 1990), is present in nearly all cell types. The regulation of cell proliferation by CD81 has been shown to be positively associated with the recruitment of the adaptor protein, Shc, to the plasma membrane and the activation of ERK/MAPK pathway (Carloni, 2004; Hemler, 2005). CD81 at the surface of B cells directly associates with CD19, a signaling molecule, and CD19 associates with the complement receptor CD21, which lacks a signaling domain. Moreover, CD81 is required for the membrane reorganization that is induced in response to co-engagement of the B-cell receptor (BCR) and CD19/CD21 complex (Levy and Shoham 2005) and this co-engagement of associated proteins is sufficient to increase the activity of the B-cell response (Levy and Shoham 2005). This did not occur in *Cd81^{-/-}* mice (Levy and Shoham 2005). CD81 has also been identified as a cell surface receptor for HCV (Pileri *et al.*, 1998). However, CD81 is required, but not sufficient, for HCV infection (McKeating *et al.*, 2004). In *D. melanogaster*, a mutant of tetraspanin gene, *late bloomer (lbm)* has been unambiguously linked to the formation of synaptic contacts at neuromuscular junctions in the embryo (Kopczynski *et al.*, 1996), and two additional tetraspanin genes also contribute to timely embryonic synapse formation (Hemler, 2005). However, deletion of 9 of the 36 tetraspanin genes in *D. melanogaster* did not cause severe developmental abnormalities (Huang *et al.*, 2005), suggesting redundancy among tetraspanins. In *C. elegans*, the TSP-15 tetraspanin protein functions to maintain epithelial integrity (Hemler, 2005). In addition to those tetraspanins found in animals, tetraspanins are also found in fungi. In the fungal plant pathogens *Magnaporthe grisea* and *Botrytis cinerea*, Mgpls1 and Bcpls1, respectively, are required for fungal penetration into the leaves of the host plant (Gourgues *et al.*, 2004; Clergeot *et al.*, 2001).

INTRODUCTION

The tetraspanins described above provide a general overview of the functions of tetraspanin proteins. These proteins are widely expressed in divergent cell and tissue types, and are implicated in diverse biological processes. A phylogenetic tree of tetraspanins has been established and shows that all tetraspanins rise from a common ancestor (Huang *et al.*, 2005), suggesting that tetraspanins are highly conserved during evolution, and moreover, that tetraspanins have a uniform architecture, suggesting that they may function with similar mechanisms.

1.4.2 Tetraspanins structural properties and the TEM

Tetraspanins are proteins containing 200-350 amino acids. The conventional tetraspanin structure consists of four transmembrane (TM) domains, two extracellular loops and short cytoplasmic N- and C-tails. The first, third and fourth TM domains often contain polar residues of unknown function, and almost all tetraspanins are post-translationally modified by the addition of palmitate to the cysteine residues proximal to the membrane. TM domains 1 and 2 flank a small extracellular loop (SEL) containing 13-30 amino acids, whereas TM domains 3 and 4 flank a large extracellular loop (LEL) containing 61-150 amino acids. The structure of the SEL has not yet been determined, but analysis of the crystal structure of a recombinant soluble form of the LEL of CD81 has determined some properties of LEL. The LEL is subdivided into a constant region that contains three α -helices (termed A, B and E), and a variable region (located between the helices B and E) that contains an almost 100% conserved CCG motif and two other absolutely conserved cysteins. The CCG motif in the LEL is characteristic of tetraspanins and is often called the 'tetraspanin signature'. The number of cysteine residues in the LEL varies considerably among tetraspanins; most contain four or six cysteine residues, and a few contain eight cysteine residues, which allows the formation of two, three or four disulfide bridges, respectively. The variable region of LEL is folded, as a result of disulfide bridges, to form a mushroom-like structure, and this region contains nearly all known tetraspanin protein-protein interaction sites (for reviews, see: Hemler, 2001; Hemler, 2003; Levy and Shoham 2005; Huang *et al.*, 2005). Distinct tetraspanin structural domains are associated with specific functions. In general, LELs mediate protein-protein interactions with laterally associated proteins and a few known ligands, TM domains mediate the stability and the dimerization of tetraspanins, and the cytoplasmic regions provide links to cytoskeletal and signaling molecules (Levy and Shoham, 2005).

INTRODUCTION

The first level of tetraspanin interactions is primary interaction — homozygous or heterozygous proteins interacting with each other directly. The CD81 LEL crystals consist of homodimers, which implies that homodimerization occurs through the LEL. In addition, the results obtained by covalent crosslinking of CD81 and CD9 indicate that tetraspanin homodimers (as well as trimers and tetramers) may be the fundamental primary units within TEMs (Levy and Shoham, 2005; Hemler, 2005). Furthermore, tetraspanin homophilic crosslinking far exceeds heterophilic crosslinking (Hemler, 2005), and tetraspanin homodimers are reported to be formed in the Golgi and have been suggested to be the common core unit for the assembly of multicomponent tetraspanin-tetraspanin and tetraspanin-partner complexes (Levy and Shoham, 2005).

The next level of tetraspanin interactions involves the assembly of primary, direct homophilic and heterophilic complexes into a network of secondary interactions (Hemler, 2005). The tendency for heterophilic association between tetraspanins is essential for this assembly. In this manner, different partner proteins can be recruited, through tetraspanins, into functionally important complexes (Hemler, 2005). Therefore, tetraspanin proteins and their associated proteins form TEMs in the plasma membrane to provide a scaffold for the transmission of external stimuli to intracellular-signaling components and to modulate biological processes (Levy and Shoham, 2005).

1.5 The aim of this project

STM plays an important event to establish the primary SAM during embryogenesis and to maintain meristem activity throughout the plant lifecycle, and it has to be shut down during the initiation of lateral organ primordia; however, little is known about its regulation. In this study, the analysis of a mutant obtained from a transcriptional effector-screen performed with a *STM:GUS* marker line following EMS mutagenesis is described. The mutant is characterised by an altered *STM:GUS* expression domain and SAM morphology. The responsible mutation was shown to be allelic to *tornado2 (trn2)* and provides evidence that plant tetraspanin-like proteins such as TRN2 contribute to SAM function. Molecular markers indicate that the size of the central stem cell zone is minor affected although the SAM is significantly enlarged compared to wild type.

2. MATERIALS AND METHODS

2.1 Plant materials and growth conditions

Arabidopsis thaliana seeds were sowed on the soil and kept at 4°C in the dark for 3 days and then transferred to a greenhouse. When elongated hypocotyls could be seen (two days after transferred to a greenhouse), the day was defined as 0 day-after-germination (0 DAG). Plants were grown on soil under 16-h-light/8-h-dark regime (long-day conditions) at 22°C.

Columbia-0 (Col) ecotype was used as the wild-type in all experiments. *clavata3-2* (*clv3-2*), *wuschel-1* (*wus-1*), *shoot meristemless-1* (*stm-1*) and *shoot meristemless-5* (*stm-5*) seeds were obtained from The European *Arabidopsis* Stock Center (NASC). *tornado1-1* (*trn1-1*), *torndo2-1* (*trn2-1*) and *tornado2-2* (*trn2-2*) seeds were a kind gift from Cnops G..

The *STM-GUS* transgenic line was created and their seeds were treated with methanesulfonate (EMS). 0.3g *STM-GUS* transgenic seeds were treated with 0.1% Tween 20 for 15 minutes and then immersed in 15 ml H₂O contains 37 µl 100% EMS overnight (Koenig 1999).

2.2 Chemicals and enzymes

All chemicals of analytical quality have been purchased from Bilmol (Hamburg), Biozyme (Hameln), Fluka (Neu-Ulm), Life Technologies (Karlsruhe), Merck-Eurolab (Darmstadt), Pharmacia (Freiburg), Roche Dianostics GmbH (Mannheim), Roth (Karlsruhe), Serva (Heidelberg) and Sigma (Dewasenhof).

Enzymes were purchased from Firmen Gencraft (Muenster), Invitrogen GmbH (Karlsruhe), New England Biolabs (Frankfurt am Main), Promega GmbH (Mannheim), Roche Diagnostics GmbH (Mannheim) and Stratagene (Heidelberg). Concentrated (10 x or 5 x) buffers were supplied with each enzyme and used according to the manuscript suggests.

Expendable materials were from Roth (Karlsruhe) and Sarstedt (Rommelsdorf).

2.3 Buffers, solutions and media

All routine used solutions and buffers for culturing *E. coli* were described before by Ausubel et al. (1996). All buffers, solutions and media were prepared with double distilled H₂O (ddH₂O, Milli-Q, Water-Clinging-System, Millipore Eschborn). Solutions used for molecular biology experiments were autoclaved or sterilized with filters (0.2 µm filter, Roth).

2.4 Bacteria and vectors

2.4.1 Bacteria strains

DH10B F⁻, endA1, Δ(mrr-hsdRMS-mcrBC), Φ80dlacZΔM15, ΔlacX74, deoR, recA1, araD139, Δ(ara, leu)7697, galU, galK⁻, rpsL, nupG (Invitrogen)

TOP 10 F⁻, mrcA, Δ(mrr-hsdRMS-mcrBC), Φ80dlacZΔM15, ΔlacX74, recA1, deoR, araD139, Δ(ara, leu)7697, galU, galK, rpsL(Str^R), endA1, nupG (Invitrogen)

2.4.2 Vectors

pCR[®]II-TOPO (Invitrogen)

2.5 Oligonucleotides

Oligonucleotides were obtained from Eurogentec (Seraing, Belgien) or Sigma (Deisenhof).

Primers used in this study of co-dominant cleaved amplified polymorphic sequences (CAPS) markers were described before by Konieczny and Ausubel (1993) or in the TAIR databank (<http://www.arabidopsis.org>).

Primer sequences for amplifying specific gene fragments for making probes of RNA *in situ* hybridization:

Gene name	Oligonucleotide sequence
<i>TRN2</i>	
Forward	ATG CCT TTA AGC AAC AAT GTA ATT
Reverse	TCA AGT ATA ACC CTG CTT GTA CT
<i>WUS</i>	
Forward	GCA TCA GCA TCA TCA TCA TCA A
Reverse	CTA GTT CAG ACG TAG CTC AAG AGA
<i>CLV3</i>	
Forward	CAG TCA CTT TCT CTC TAA AAA TGG
Reverse	TCA AGG GAG CTG AAA GTT GTT T
<i>LFY</i>	
Forward	ATG GAT CCT GAA GGT TTC ACG AG
Reverse	CTA GAA ACG CAA GTC GTC GC

For *STM* RNA *in situ* hybridization, the probe was described before by Long et al., (1996).

Primer sequences for amplifying gene fragments for genotyping:

Gene name	Oligonucleotide sequence
<i>trn2₃₀₁₀</i>	
Forward	CAC TTA ATC AGT CAC GCC GAA CTA C
Reverse	GAC GAT AAT CAA TCC GAT AAG C
<i>stm-1</i>	
Forward	GTC AAT TCA AAT CCC TCT CTC TA
Reverse	GCT TTC CTT TCT TCC TCT TCT TC
<i>stm-5</i>	
Forward	GAA GAA GAG GAA GAA AGG AAA GC
Reverse	GCA ATG CCA ACA TGA GCT AAC

wus-1

Forward	GCA AGC TCA GGT ACT GAA TGT G
Reverse	CCT CCA CCT ACG TTG TTG TAA TTC

clv3-2

Forward	TCC GGT CCA GTT CAA CAA CT
Reverse	CTC CCG AAA TGG TAA AAC

Primers for real-time PCR were designed by Applied Biosystems (TaqMan® Gene Expression Assays). A non-inventoried assay At02329915_s1 (*ACTIN 2*) was used as an endogenous control, but the sequences of primers were not given.

Primer and probe sequences for real-time PCR:

Gene name	Oligonucleotide sequence
<i>STM</i>	
Forward	GCC GCT TAT GTC AAT TGT CAG AA
Reverse	GAC GAG CAT GCC TCC TCT AG
Probe	FAM CCA CCG GAG GTT GTG NFQ
<i>WUS</i>	
Forward	GGA TCA TCA TTA CTC ATC TGC ACC TT
Reverse	GCC ACC ACA TTC TTC TTC TTC TTG A
Probe	FAM TTC GAT AGA GCA AAG CCT NFQ
<i>CLV3</i>	
Forward	CAG ATC TCA CTC AAG CTC ATG CT
Reverse	CCA ACC CAT TCA CTT TCC ATT TTC A
Probe	FAM ACG TTC AAG GAC TTT CC NFQ

FAM, 6-carboxy-fluorescein.

NFQ, nonfluorescent quencher.

2.6 Genetic mapping

The mapping work was carried out by using CAPS markers (Konieczny and Ausubel, 1993).

Heterozygotes of the interesting line (Colombia ecotype), which was isolated from the mutagenesis screen, were crossed to Landsberg *erecta* plants. 30 mutant plants of the F2 population were picked up, and the genomic DNA was extracted. DNA fragments of CAPS markers were amplified by polymerase chain reaction (PCR) by using specifically designed primers distributed over the genome of *Arabidopsis* (Konieczny and Ausubel, 1993, TAIR databank). To identify restriction fragment length polymorphism (RFLP) between the amplified Col and *Ler* sequences, the PCR products were digested with specific endonucleases (Konieczny and Ausubel, 1993, TAIR database), and the ecotype of origin of these sequences could thus be determined. The mutant locus then could be unambiguously mapped to one of the 10 *Arabidopsis* chromosome arms.

2.7 Molecular biology methods

2.7.1 Standard molecular biology methods

All molecular biology standard methods were described before (Ausubel et al., 1996). Other materials (enzymes and chemicals) were described above.

2.7.2 Transformation of bacteria (*E. coli*)

Electrocompetent *E. coli* was used for transformation (Muehlhardt, 2000). 50 μ l Electrocompetent *E. coli* with 1 μ l vector was added into a pre-cooled 0.1 cm electroporation cuvette and then placed in a *GenePulser*TM (BIORAD). The condition for electroporation was: capacity 25 μ F, voltage 1.8 kV, and resistor 200 Ω .

2.7.3 Preparation of plasmid DNA

“Alkaline lysis protocol” (Sambrooke et al., 1989) was used for plasmid-mini preparation. Large amount of DNA or DNA-probes for sequencing or *in situ* hybridization were prepared by the kits (Plasmid Midi or Maxi kit, Qiagen).

2.7.4 The extraction of the genomic DNA from *Arabidopsis thaliana*

Up to 200 mg plant tissues (1-2 young leaves or 3-4 inflorescences) were harvested and placed in a 1.5 ml tube and frozen immediately with liquid nitrogen. The tissue was crushed by a micropistil against the tube wall. After crushing, 600 μ l EB-buffer (100 mM Tris pH 7, 50 mM EDTA, 500 mM NaCl. Add 2 μ l RNase (10 μ g/ μ l) and 12 μ l β -mecaptoethanol into the EB buffer before use) was added and the tube was vigorously vortexed to suspend the sample powder. After vortexing, added 40 μ l 20% SDS (mixed well, did not vortex) and 200 μ l 5M KAc (mixed well). The tube was incubated at 68°C for 15 minutes to homogenize the tissue and then placed on ice for 20 minutes. Centrifuged the tube at full speed for 2 minutes. Removed the supernatant to a new 1.5 ml tube and added 0.6 volume isopropanol into the supernatant and mixed well. To precipitate genomic DNA, centrifuged the tube at full speed for 5 minutes, and then washed the pellet by 70% EtOH. Slightly dried the pellet and dissolved it in 50 μ l TE buffer. The genomic DNA was then stored at 4°C for several months.

2.7.5 The extraction of total RNA from *Arabidopsis thaliana* and the synthesis of *cDNA*

The RNeasy Plant Mini Kit (QIAGEN) was used to extract total RNA of *Arabidopsis thaliana*. On-column DNA digestion was performed during RNA purification. 500 ng – 2 μ g total RNA was used to synthesize *cDNA*. Oligo(dT) was used to hybridize to 3' poly(A) tails, which were found in the vast majority of eukaryotic mRNAs. SuperScriptII™ reverse transcriptase (Invitrogen) was used to synthesize cDNAs at 48°C for one hour. After RNaseH treatment, *cDNA* was used as templates for real-time PCR.

2.7.6 Polymerase chain reaction (PCR)

In a standard PCR reaction, 100 pg to 10 ng DNA was used as the template. 1-2 U *Taq*-polymerase (Invitrogen) was added to the reaction mixture (1X PCR reaction buffer, 1.5 mM MgCl₂, 0.2 mM dNTP, 0.2-1.0 μM primers). The final volume of the reaction mixture was 50 μl. The polymerase chain reaction was taken place in a MJ Research Thermoblock (Biozyme, Hameln) using the following program:

- 1 Initial denaturation: 1 minute 94°C
- 2 Denaturation: 30 seconds 94°C
- 3 Annealing: 30 seconds at the appropriate temperature of the primer pairs
- 4 Elongation: 1 minute/kb PCR fragment at 72°C
- 5 Cycle number: repeat 2-4 for 39 times
- 6 Final elongation: 10 minutes at 72°C
- 7 Pause 4°C forever

2.7.7 Real-time RT-PCR

2.7.7.1 The principle of real-time PCR

The real-time PCR system is based on the detection and quantitation of a fluorescent reporter. This signal increases in direct proportion to the amount of PCR product in a reaction. By recording the amount of fluorescence emission at each cycle, it is possible to monitor the PCR reaction during exponential phase where the first significant increase in the amount of PCR product correlates to the initial amount of target template. The higher the starting copy number of the nucleic acid target, the sooner a significant increase in fluorescence is observed. A significant increase in fluorescence above the baseline value measured during the 3-15 cycles (usually the exponential phase) indicates the detection of accumulated PCR product.

A fixed fluorescence threshold is set significantly above the baseline that can be altered by the operator. The parameter Ct (cycle threshold) is defined as the cycle number at which the fluorescence emission exceeds the fixed threshold. Ct is the most important parameter for quantitation. The higher the initial amount of genomic DNA, the sooner accumulated product is

MATERIAL AND METHODS

detected in the PCR process, and the lower the Ct value. The threshold should be placed above any baseline activity and within the exponential increase phase (which looks linear in the log transformation). The log phase provides the most useful information about the reaction. Some software allows determination of the cycle threshold (Ct) by a mathematical analysis of the growth curve. This provides better run-to-run reproducibility. A Ct value of 40 or higher means no amplification and this value cannot be included in the calculations. Besides being used for quantitation, the Ct value can be used for qualitative analysis as a pass/fail measure. To calculate the relative change of a gene in different samples, Ct values have to be normalized. A simple way to normalize Ct values is that using the Ct value of the targeted gene to minus the Ct value of the reference gene, and the normalized Ct is called delta Ct. Delta Ct can be used to compare changes of gene expression directly or to calculate the relative expression change of a gene between two samples (Livak and Schmittgen, 2001).

TaqMan probes are oligonucleotides longer than the primers (20-30 bases long with a T_m value of 10°C higher) that contain a fluorescent dye usually on the 5' base, and a quenching dye typically on the 3' base. When irradiated, the excited fluorescent dye transfers energy to the nearby quenching dye molecule rather than fluorescing (this is called FRET = Förster or fluorescence resonance energy transfer) (Hiyoshi, 1994; Chen, 1997). Thus, the close proximity of the reporter and quencher prevents emission of any fluorescence while the probe is intact. TaqMan probes are designed to anneal to an internal region of a PCR product. When the polymerase replicates a template on which a TaqMan probe is bound, its 5' exonuclease activity cleaves the probe (Holland, 1991). This ends the activity of quencher (no FRET) and the reporter dye starts to emit fluorescence which increases in each cycle proportional to the rate of probe cleavage. Accumulation of PCR products is detected by monitoring the increase in fluorescence of the reporter dye (note that primers are not labeled). TaqMan assay uses universal thermal cycling parameters and PCR reaction conditions. Because the cleavage occurs only if the probe hybridises to the target, the origin of the detected fluorescence is specific amplification. The process of hybridization and cleavage does not interfere with the exponential accumulation of the product. One specific requirement for fluorogenic probes is that there be no G at the 5' end. A 'G' adjacent to the reporter dye quenches reporter fluorescence even after cleavage. Well-designed TaqMan probes require very little optimisation.

Relative gene expression comparisons work best when the gene expression of the chosen

MATERIAL AND METHODS

endogenous/internal control is more abundant and remains constant, in proportion to total RNA, among the samples. By using an invariant endogenous control as an active reference, quantitation of an mRNA target can be normalised for differences in the amount of total RNA added to each reaction. For this purpose, the most common choices are 18S RNA, GAPDH (glyceraldehyde-3-phosphate dehydrogenase) and β -actin. Because the 18S mRNA does not have a poly-A tail, cDNA synthesis using oligo-dT should not be used if 18S RNA will be used as a normaliser. GAPDH is severely criticised as a normaliser (Dheda, 2004). Caution should also be exercised when 18S RNA is used as a normaliser as it is a ribosomal RNA species (not mRNA) and may not always represent the overall cellular mRNA population. Since the chosen mRNA species should be proportional to the amount of input RNA, it may be best to use a combination as normaliser. It is desirable to validate the chosen normaliser for the target cell or tissue. It should be expressed at a constant level at different time points by the same individual and also by different individuals at the target cell or tissue. It is important to choose a normalizer whose expression will remain constant under the experimental conditions designed for the target gene. The strategy of using multiple and variable normaliser genes depending on the cell and tissue type is validated for general use.

2.7.7.2 Preparation and manipulation of real-time RT-PCR

In this study, primers and probes for target genes were ordered, and designed by Applied Biosystems (TaqMan® Gene Expression Assays) (see nucleotides part). Primers and probes were mixed in the stock solutions. Oligonucleotides were at 100mM and had to be diluted to 1/20 when used. The stock solution should be aliquoted, frozen and kept in the dark. *cDNAs* were diluted to 1/8 for real-time PCR reactions to quantify *STM* and *LFY* expressions and to 1/4 for real-time PCR reactions to quantify *WUS* and *CLV3* expressions. *ACT2* was used as an endogenous control for each reaction.

Fifteen 11-DAG-old seedlings of Columbia and mutant plants were collected, and the total RNA was extracted. The amount of the total RNA was measured by a spectrophotometer using UV-260, and the ratio of A260/A280 was determined and should be between 1.8 and 2.2 to qualify the total RNA for making *cDNA*. Same amounts of the total RNA of wild-type and mutant plants were taken, and reverse transcriptions were carried out to make *cDNAs*. The *cDNA* was first tested by a normal PCR reaction using designed *ACT2* primers, and the PCR product was

MATERIAL AND METHODS

observed by an electrophoretic gel. There had to be a single band of the PCR product of *ACT2* and no obvious differences between the wild-type and the mutant. The *cDNA* was then ready for real-time PCR reactions. The reaction mixture was prepared as follows: 4 μ l TaqMan® Universal PCR Master Mix, diluted primer solution and appropriately diluted *cDNA*. The final volume of the reaction mixture is 8 μ l. The reaction mixture was added into a 384-well plate, and real-time PCR reactions were taken place in an ABI Prism HT7900 machine (TaqMan®). SDS software version 2.2.1 (TaqMan®) was used for controlling each real-time PCR reaction. Ct values comparisons and t-tests were done by Excel software (version 11.1.1, Microsoft® Excel 2004 for Mac). Relative gene expression changes were compared by using the formula described before (Livak and Schmittgen, 2001). Real-time PCR reactions were repeated 4 times using 4 independently prepared *cDNAs* from 4 independently collected wild-type and mutant plants.

2.7.8 Non-radioactive RNA *in situ* hybridization

Full length *cDNA* fragments (*TRN2*, *STM*, *CLV3*, *WUS* and *LFY*) were amplified by primers described above and then cloned into pCR®II-TOPO (invitrogen) vectors. Vectors were linearized by appropriate enzymes and anti-sense RNA probes were then transcribed by SP6 or T7 polymerase.

Nonradioactive *in situ* hybridization experiments were performed essentially as described before (Bradley et al. 1993).

2.8 Histology

2.8.1 Fixation, embedment and sections of the plant tissue

2.8.1.1 Preparation of the fixative

4 g paraformaldehyd was dissolved in 100 ml pre-heated 1XPBS (pH=11) (10X PBS: 1.3 M NaCl, 0.07 M Na₂HPO₄, 0.03 M NaH₂PO₄). Placed the solution on ice till it decreased to room temperature, and then adjusted the pH value to 7 with concentrated H₂SO₄. Added 200 μ l Tween20 to the fixative and kept it on ice.

2.8.1.2 Fixation of samples

To fix young seedlings or inflorescences, leaves must be removed. 20 samples could be putted into a 20 ml glass bottle filled with the fixative. 3 X 10 minutes vacuum-infiltration was performed till all samples were sunk, and then putted the fixed samples at 4 °C overnight.

2.8.1.3 Embedment of samples

After fixation, exchanged the fixative for cold EtOH and performed series dehydration in 50%, 70%, 85% cold EtOH, each for 90 minutes. After serious dehydration, exchanged EtOH for 0.1% Eosin Y (dissolved in 100% EtOH), and putted the solution at 4 °C overnight. In the next day, exchanged the solution for fresh 0.1% Eosin Y and putted it on ice for 90 minutes. After Eosin Y, exchanged the solution for 100% EtOH, 50% EtOH/50% Rotihistol and three times 100% Rotihistol, each for 60 minutes. After 100% Rotihistol, exchanged the solution for solution of 50% (v/v) fresh Rotihistol and 50% (v/v) Paraplast Pius[®], and then putted the solution at 50 °C overnight. In the next three days, exchanged the solution for fresh molten Paraplast Pius[®] in the mornings and evenings, and putted the solution at 60 °C.

After three days solutions exchanges, samples had to be embedded into a wax block. A model within some molten Paraplast Pius[®] was placed on a warm plate (60 °C). Molten Paraplast Pius[®] within samples was then poured into the pre-warmed model, and fresh molten Paraplast Pius[®] was added to cover all samples. Used a pre-heated tweezers to adjust samples to appropriate orientations, and then carefully putted the model in cold water. After solidification, the wax block was stored at 4 °C for several months.

2.8.1.4 Sections

The sample-containing wax block was cut to be a cube with 1.5 cm side length. 7 µm thick sections were made by the microtome (Leica: Disposable microtome blade 819), and ribbon pieces were floated on a Superfrost plus slide (Menzel-Gläsner / KEBO 113.720-0) covered with distilled H₂O. Placed the slide on a slide warmer (42 °C) for 5 minutes to allow the ribbon to

flatten out and then removed H₂O. Slides should not be kept on the warmer more than one day. After slides complete dried, stored them at room temperature or 4°C.

2.8.2 Microscopic technique

Light microscopy was performed with an *Axioskop* microscope with Nomarsky-Optik (Zeiss, Heidelberg, Germany) and an *Axiocam* camera (Zeiss, Heidelberg, Germany) was used. The DISKUS software package (Carl H. Hilgers-technwasches Buero, Koenigswinter, Germany; version 4.30.578) was used to take digital photos.

2.8.3 GUS staining

GUS-activity was assayed according to Sessions and Yanofsky, 1999. To allow complete penetration of the X-gluc-solution, plants were vacuum-infiltrated in staining buffer (0.2% Triton X-100, 50mM NaPO₄ pH 7.2, 2mM potassium-ferrocyanide K₄Fe(CN)₆*H₂O, 2mM potassium-ferricyanide K₃Fe(CN)₆ containing 2mM X-Gluc) for 15 to 30 minutes and afterwards incubated at 37°C from 5 minutes to overnight (the staining time was dependent on each individual transformed line). Clearing was performed by series dehydration in 50%, 70%, 85%, 95% and 100% Ethanol, each for 1 hour.

2.9 Computer analysis

The analyses of DNA and protein sequences were done by programs offered by Biology Workbench 3.2 (<http://seqtool.sdsc.edu/CGI/BW.cgi>). Primers were designed by the program Launch NetPrimer (<http://www.premierbiosoft.com/netprimer/netprlaunch/netprlaunch.html>). Chi squer values were calculated by the web Chi squaer calculator (http://www.georgetown.edu/faculty/ballc/webtools/web_chi.html). Sequences were obtained from databanks of NCBI (<http://www.ncbi.nlm.nih.gov/>) and TAIR (<http://www.arabidopsis.org>).

3. RESULTS

3.1 Identification of the mutant

To search for *STM* effector genes, an EMS-mutagenesis screen was previously carried out on a homozygous *STM:GUS* line (Kirch *et al.*, 2003) where glucuronidase (GUS) activity reflected the activity of the *STM* promoter in the shoot meristem. The GUS activity in shoot tips represented the *STM* expression (Fig. 1), and changes in the GUS pattern therefore reflected affected *STM* activity. After self-fertilization of M1 progeny, the M2 generation was screened for differences in GUS expression at the early seedling stage. Among 4,900 independent M2 lines, two lines, line 3010 and 145 showed expansion of GUS activity domains in shoot tips of young seedlings, and they were subjected to further analyses.



Figure 1. The GUS activity in the shoot tip represents *STM* expression of a *STM:GUS* transgenic plant. (A) A *STM:GUS* young seedling shows the GUS stain in the shoot tip (red arrow). In this figure, one leaf in front was removed to make the shoot tip be clearly seen. The domain of GUS activity is consistent with the *STM* expression pattern, which is confined in the meristem.

Mutant plants of line 3010 displayed a unique phenotype of twisted organs (see the description of the phenotype below) and the population showed segregation ratios conforming to the 3:1 pattern that would be expected for a recessive single mutation. Furthermore, this phenotype was linked to the expanded GUS domain in mutant shoot tips (Fig. 2A). To understand the effects on the mutant SAM, serially longitudinal sections of wild-type and mutant seedlings were made and compared. The SAM of seedlings that are younger than one week old did not show obvious

RESULTS

discrepancies between wild-type and mutant seedlings. However, sections of 11-DAG-old mutant seedlings showed vast effects in the morphology of the SAM (Fig. 2C). Seventy-five percent of 11-DAG-old mutants had an enlarged and protruding SAM at the apex of the shoot, whereas the wild-type SAM was smooth and dome-shaped (Fig. 2B and C).

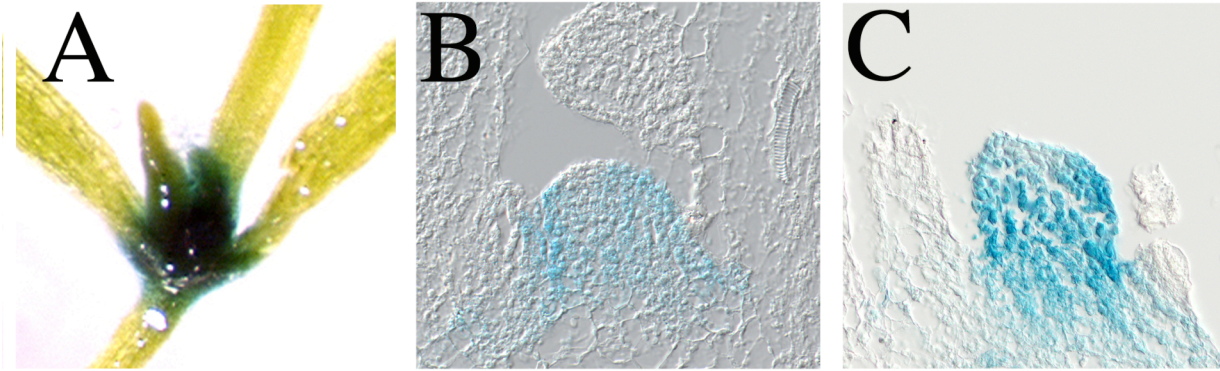


Figure 2. GUS stains in shoot tips of wild-type and homozygous 3010 mutant young seedlings. (A) A 7-DAG-old homozygous 3010 mutant seedling shows expanded GUS activity at the shoot tip. **(B)** The longitudinal section of a 11-DAG-old *STM:GUS* seedling reveals that the GUS stain is confined in the dome shaped SAM. **(C)** The longitudinal section of a 11-DAG-old homozygous 3010 mutant seedling reveals that the GUS stain is confined in the aberrant SAM, which is protruding and enlarged compared to wild-type **(B)**.

Like homozygous mutants of the line 3010, mutant plants of the line 145 also had expanded GUS domain readily detected in shoot tips of young mutant seedlings (Fig. 3 A). However, at least two phenotypes, tiny-white plants and three cotyledons plants (Fig 3 B and C), were segregating in 145 populations during propagation. In addition, the linkage between mutant phenotypes and the expanded GUS domain was uncertain. Because the line 145 did not show a segregation pattern compatible with a single locus trait or a double mutant combination, further analysis therefore focused on the line 3010, which is described in this study.



Figure 3. Two phenotypes segregating in the line 145. (A) The young mutant seedling of the line 145 shows the GUS activity at the shoot tip not restricted to the SAM but expanded to leaf primordia. (B) and (C) at least two phenotypes segregating in the M3 population.

3.2 The mutant phenotype of the line 3010

3.2.1 The morphology of the mutant

Homozygous mutant 3010 plants are severely dwarfed, have twisted and malformed organs, and are sterile. Because of the sterility, this line was maintained and propagated heterozygously. Although homozygous 3010 seedlings did not show any obvious phenotype that could be observed by the naked eye in hypocotyls and cotyledons, mutant seedlings could be unambiguously identified after the emergence of the first pair of true leaves (Fig. 4A and B). Mutant leaves had irregular margins and asymmetric leaf blades, and were reduced in size (Fig. 4C and D). In some cases, rosette leaves rotated 180° during development and hence the abaxial and adaxial sides were turned to the opposite directions. Interestingly, leaves usually lost half of the lamina, and in the most severe cases they lost their entire lamina and became pin-like structures (Fig. 4D, arrow head). Unlike wild-type leaves that have centrally located midribs, mutant leaves had thicker midribs, located near the center, or bifurcated ribs located marginally (Fig. 4F).

The twisted phenotype was not restricted to the vegetative phase but involved cauline leaves, the inflorescence stem, flowers and siliques (Fig. 4H-K). Mutant flowers were also twisted, asymmetric and smaller when compared with wild-type, and were accompanied by reduced numbers of floral organs in the outer 3 whorls (Table 1). This effect was least pronounced in the

RESULTS

whorl of sepals (3.2 as compared with 4 in wild-type), but the number of petals was reduced to 2.4 (compared with 4 in wild-type) and, on average, mutant flowers had only 3.5 stamens compared with 6 in wild-type (summarized in Table 1). In contrast with the outer three whorls, there were two carpels at the mutant flower center, same as the wild-type flower, suggesting that the number of carpels was unaffected. However, 52% of the mutant flowers had carpels that were not fused on their upper parts, whereas wild-type flowers always had a central style with well-fused carpels. Mutant stamens occasionally generated little sterile pollen, and thus, both male and female sex organs are defective in mutant flowers.

Table 1. The mean of floral organs

	Sepals	Petals	Stamens	Carpels	Flower having style with unfused Carpels
WT (n=31)	4.0 ± 0	4.0 ± 0	6.0 ± 0	2.0 ± 0	0.0%
<i>trn2₃₀₁₀</i> (n=39)	3.2 ± 0.8	2.4 ± 0.8	3.5 ± 1.0	2.0 ± 0	52.0%

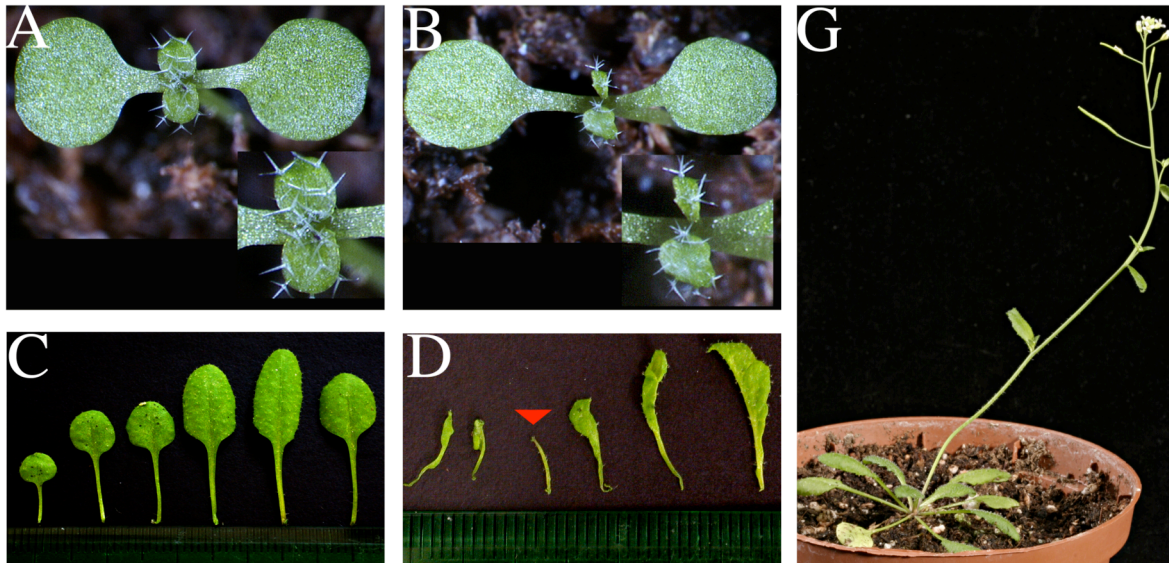


Figure 4. The homozygous 3010 mutant plant shows pleiotropic phenotype. (A) A 7-DAG-old Columbia wild-type seedling compared to (B), a 7-DAG-old homozygous 3010 mutant seedling, which shows the first pair of true leaves smaller and twisted (see enlargements in (A) and (B)). (C) The first to sixth rosette leaf of Columbia wild-type compared to (D), the first to sixth rosette leaf of the homozygous 3010 mutant. The mutant leaves are twisted, reduced in size, and half of leaf laminas are usually missing. In the most severe case, leaves developed to a pin-like structure (red arrow head).

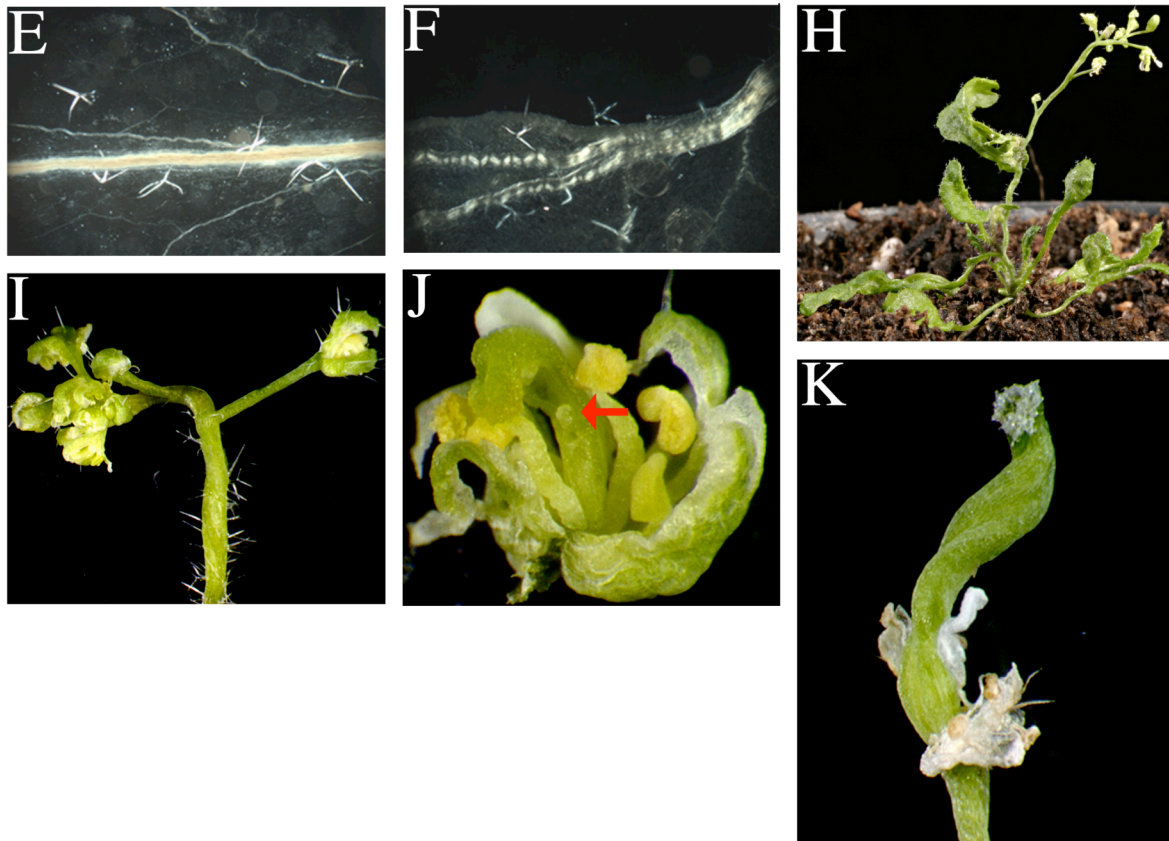


Figure 4. (Continued) (E) The wild-type leaf has a midrib located centrally. (F) The mutant leaf usually has a broadened midrib located centrally or a bifurcated midrib as shown in the figure located marginally. (G) One-month-old Columbia wild-type plant. (H) The one-month-old mutant plant is dwarf compared with wild-type. (I) The shoot of the homozygous 3010 mutant is also twisted and with small and malformed flowers. (J) The mutant flower is asymmetric and has fewer floral organs in the first to third whorl, and a style with unfused carpels at the floral center (red arrow). (K) The mutant silique is also twisted and occasionally produces few sterile seeds.

3.2.2 The plastochron index and the flowering time of the mutant

The plastochron index was calculated from 11 wild-type and mutant plants for 9 days. On average, wild-type plants took 1.81 ± 0.14 days to initiate two leaf primordia successively, whereas mutant plants took 2.38 ± 0.24 days (Fig. 5A). When plastochron indexes were compared, the Student's *t*-test gave a *p* value of 0.026, suggesting that mutants initiate leaves significantly more slowly than wild-type plants. Despite the leaf initiation rates, mutants

RESULTS

flowered earlier than wild-type plants. On average, wild-type plants flowered at 25.1 DAG, whereas mutants flowered at 20.7 DAG. Furthermore, wild-type plants had 12 leaves, whereas mutants had only 9.1 leaves, while bolting (Fig. 5B). The Student's *t*-test gave *p* values much smaller than 0.001, suggesting that mutants flower significantly earlier than wild-type plants.

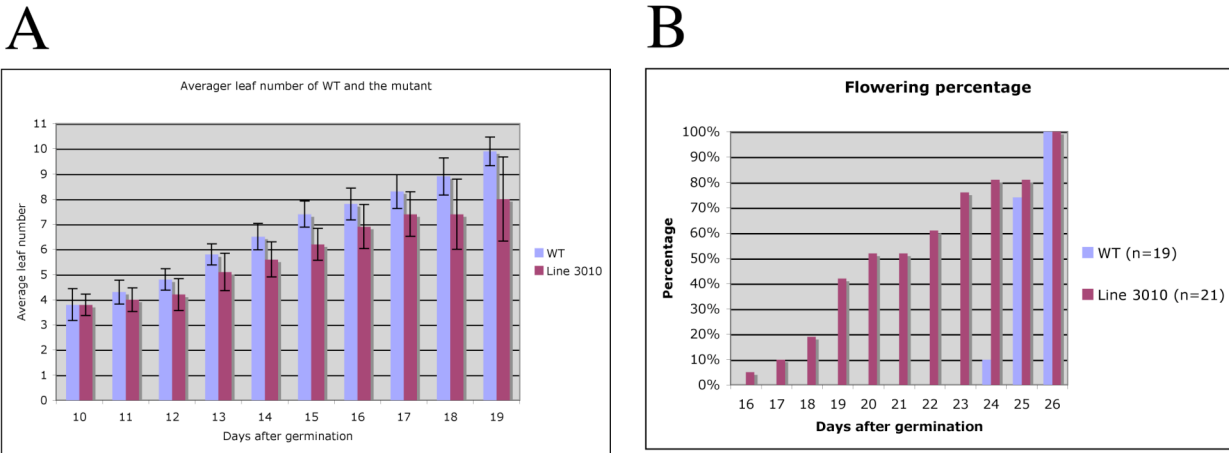


Figure 5. The average leaf number and flowering time of the wild-type plants and the homozygous 3010 mutant plants. (A) The average leaf number of mutant plants was smaller than of wild-type. The plastochron indices were calculated for both wild-type and mutant plants and showed that mutants initiated leaf primordia slower than wild-type. (B) Mutants start to flower at 16 DAG and have a wide window of time to flower. The average time to flower of mutants is earlier than of wild-type plants, in addition, the average leaf number of mutants is smaller than of wild-type plants while flowering (see text).

To summarize, the homozygous mutant 3010 plants have a pleiotropic phenotype that affects stature, leaves, inflorescence shoots, flowers, leaf initiation rates and flowering time. The pleiotropic phenotype implies that the mutated locus may affect meristem function or the gene is widely expressed and implicated in different developmental processes.

3.3 Genetic mapping and allelism test

Genetic mapping was carried out by using CAPS markers that were distributed across the entire *Arabidopsis* genome. Four CAPS markers (*LMYC6*, *MDA7*, *EG7F2* and *ATTED2*) on the long arm of chromosome 5 were tightly linked with the mutant phenotype. The marker *LMYC6* showed 90% linkage with the mutant phenotype and the marker *MDA7*, which is more telomeric than the marker *LMYC6*, showed 100% linkage with the mutant phenotype (Fig. 6A and B). This

RESULTS

result indicated that the mutant locus should be located in the area between markers *LMYC6* and *MDA7* (Fig. 6C). Therefore, the chromosomal position of the mutant locus was assigned to the long arm of chromosome 5, close to the CAPS marker *MDA7*.

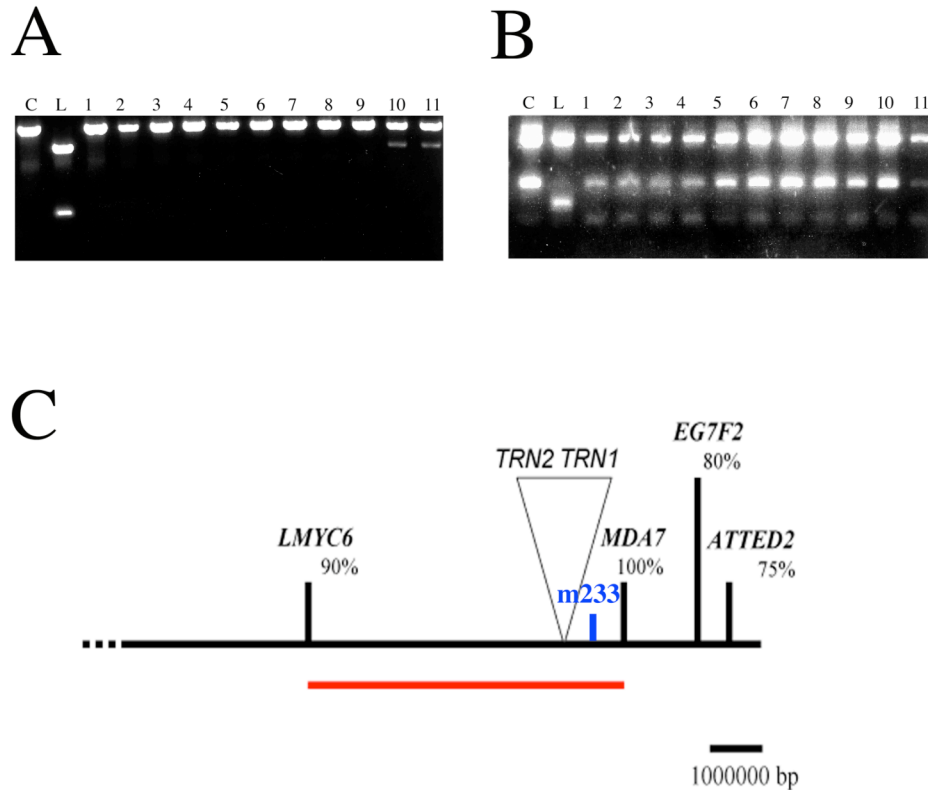


Figure 6. Genetic mapping of the mutant locus. (A) and (B) show the segregation of the mutant locus in F2 progeny from the heterozygote of the mutant line 3010 (Col background) X Landsberg *erecta* crosses. PCR amplified CAPS marker *LMYC6* was digested by *HindIII* (A) and *MDA7* was digested by *AluI* (B). The most left two lanes in both figures correspond to Col (C) and *Ler* (L) ecotype. The doublet bands are readily apparent in the heterozygotes. The marker *LMYC6* shows 90% linkage and the marker *MDA7* shows 100% linkage to the mutant locus. (C) The mutant locus was assigned to the area between CAPS markers *LMYC6* and *MDA7* (red line). *TRN1* and *TRN2* genes were mapped to the same area close to the marker *MDA7*. The RFLP marker m233 (blue) is near the CAPS marker *MDA7*. Centromere is to the left.

The phenotype of homozygous 3010 mutant plants was reminiscent of the previously described mutants, *trn1* and *trn2* (Fig. 7A and B). *TRN1* was mapped to the bottom half of the long arm of

RESULTS

the chromosome 5, close to the visible marker *tz* and the RFLP marker m233 (Cnops *et al.*, 1996). Genetic linkage between *TRN2*, and the DFR, AthPHYC and Ath50191 markers, indicated that *TRN2* is also located on the same area of the chromosome 5 — most likely on the left of *TRN1* (Fig. 6C) (Cnops *et al.*, 1996; 2000). Based on the genetic map of chromosome 5, the RFLP marker m233 is near the CAPS marker *MDA7* (Fig 6C). Therefore, both *TRN1* and *TRN2* genes should be located in the area enclosed by the markers *LMYC6* and *MDA7* (Fig. 6C). As the homozygous 3010 mutant and the *trn* mutants had similar phenotypes, and the mutant loci were mapped to the same area, it was then examined whether the 3010 mutant locus is allelic to *trn1* or *trn2*.



Figure 7. *trn* mutants show similar phenotypes to the homozygous 3010 mutants. (A) and (B) are one-month-old *trn1-1* and *trn2-1* mutants, respectively. Both mutants show dwarf statures, twisted organs and sterility. The phenotypes are similar to homozygous 3010 mutant plants (compared to Fig 4 H).

To test for allelism, heterozygotes of line 3010 were crossed to heterozygotes of *trn1-1* and *trn2-1*. Based on Mendelian genetics, it is expected that a quarter of plants in the F1 population will show the mutant phenotype when mutations in two different strains reside in the same gene. The F1 population of line 3010 X *trn1-1* crosses revealed that there were no plants showing the mutant phenotype, indicating that the mutant 3010 locus and *trn1-1* are not allelic. Conversely, a quarter plants of the progeny of line 3010 X *trn2-1* crosses exhibited the mutant phenotype, strongly suggesting that the mutant 3010 locus and *trn2-1* are allelic. To further confirm that line 3010 contains a mutant *trn2* gene, both the *TRN1* and *TRN2* coding sequences were amplified by PCR from the homozygous mutant 3010 genomic DNA and subjected to DNA sequence analysis (the DNA sequence analysis was done by Gerda Cnops, Gent). The sequencing results revealed

that the homozygous mutant 3010 plants contain a wild-type *TRN1* gene but the *trn2* gene has a point mutation that is identical to one previously described in *trn2-2* (Cnops *et al.*, 2000). These results suggested that the mutant locus is an allele of *TRN2*, and the allele is hereafter referred to as *trn2*₃₀₁₀.

3.4 The *TRN2* gene encodes a tetraspanin-like protein

The *TRN2* coding region consists of two exons that are separated by a large intron of 595 bp and encodes a protein of 269 amino acids. NCBI blastp and Pfam HMM searches revealed that TRN2 has homology to the putative senescence-associated protein 5 of day lily (*Hemerocallis fulva*) and a conserved domain related to tetraspanin family at N-terminus (this study and Cnops *et al.*, 2006). Further protein sequence analysis revealed that TRN2 possesses typical features of tetraspanins: short cytoplasmic N- and C- termini, four transmembrane domains, a small extracellular loop (SEL), and a large extracellular loop (LEL) within a set of conserved cysteins (see Fig. 8A; this study and Olmos *et al.*, 2005, Cnops *et al.*, 2006). Although it contains many structural properties of tetraspanins, almost no similarity alignments could be made between TRN2 and tetraspanins. The most notable difference between TRN2 and tetraspanins is the absence of a so-called tetraspanin signature CCG in the LEL (Fig. 8A). Instead, TRN2 has a GCC motif conserved in plant homologues in the LEL (Huang *et al.*, 2005; Fig. 8B). Despite this discrepancy, TRN2 is closer to tetraspanins than to other TM4 proteins (proteins with four transmembrane domains). Therefore, TRN2 is considered to be a plant tetraspanins (Huang *et al.*, 2005) — a so-called tetraspanin-like protein.

*trn2*₃₀₁₀ has a G to A nucleotide exchange that is consistent with a point mutation induced by EMS. This nucleotide exchange in the second exon leads to a single amino acid substitution (Gly to Glu) at position 81 of TRN2, and this substitution is located on the variable region of LEL (just after a conserved cystein, which is six amino acids after the conserved GCC motif).

3.5 RNA *in situ* hybridization of *TRN2* and other meristem-related genes

3.5.1 The *TRN2* expression pattern

The expression pattern of *TRN2* was examined by RNA *in situ* hybridization using a full-length cDNA probe that is specific to *TRN2*. During vegetative development, *TRN2* transcripts were detected in the SAM through the L1 to L3 layer (Fig. 9) and preferentially in the distal tip of the leaflet and the incipient vascular tissues (Fig. 9, arrow and arrow head, respectively).

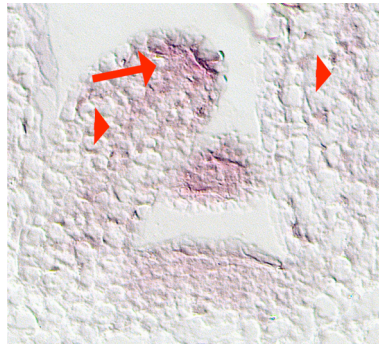


Figure 9. *TRN2* is expressed in the SAM, leaf primordia and incipient vascular strands. The longitudinal section of a 11-DAG-old wild-type seedling hybridized with the antisense RNA probe of *TRN2*. *TRN2* is expressed in the SAM through L1 to L3 layer. *TRN2* RNA accumulates also in the tip of the leaflet (red arrow) and in the incipient vascular strand (red arrow head).

After floral transition, *TRN2* transcripts accumulated in inflorescence and floral meristems (Fig. 10A). Continuous *TRN2* expression was detected through the floral meristem into the flanking sepal primordia in a stage 5 flower (Fig. 10B). In a stage 8 flower, the transcripts were detected preferentially in developing petals, anthers and the gynoecium (Fig. 10C). In later stages, strong expression of *TRN2* was observed in haploid pollen but not in tapetum layers (Fig. 10D and E). After floral organs were differentiated, *TRN2* transcripts were not detectable (Fig. 10F).

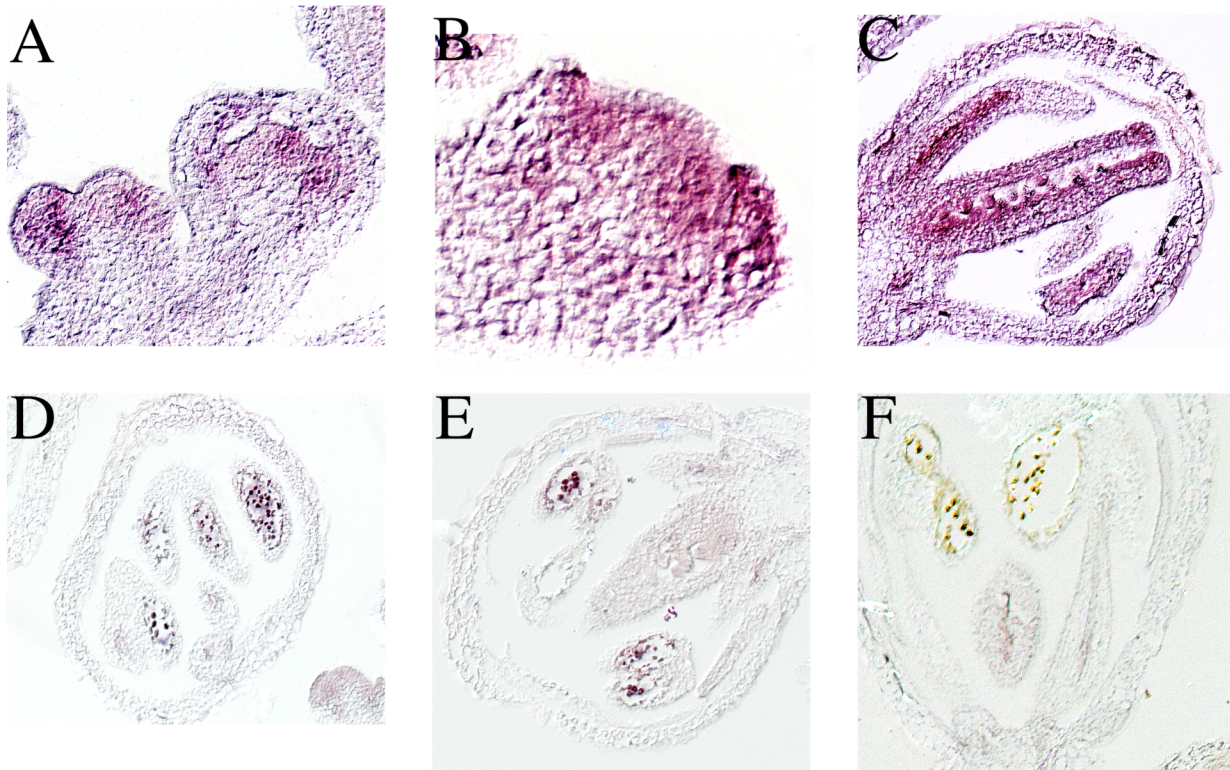


Figure 10. *TRN2* is expressed in the inflorescence meristem and developing flowers. (A) *TRN2* is expressed in inflorescence meristems, floral meristems and developing flowers. (B) A close look to a stage 5 flower. *TRN2* is expressed in the floral meristem and sepal primordia. (C) A close look to a stage 8 flower. *TRN2* is expressed in developing petals, anthers and carpels but not in sepals, which are already differentiated. (D) and (E) In a stage 10 flower, *TRN2* is expressed in the developing haploid pollen but not in tapetum layers. (D) The longitudinal section of a stage 10 flower. (E) The cross section of a stage 10 flower. (F) In a mature flower, *TRN2* expression is not detectable by RNA *in situ* hybridization.

In summary, *TRN2* transcriptional activity was detected in all types of meristem — vegetative, inflorescent and floral. *STM* is also active in these meristems (see below, Fig. 11A and B). As *TRN2* and *STM* expression spatially overlaps, defects in *TRN2* function may affect *STM* expression. However, in contrast with *STM*, *TRN2* transcripts are not confined to the meristems and are also detected in lateral primordia.

3.5.2 *STM* expression pattern in *trn2* mutants

As previously described, the expansion of the *STM-GUS* activity domain in the shoot tips of *trn2* seedlings implied an increased domain of *STM* expression. To gain insight into the effects of *STM* expression on *trn2* seedlings, RNA *in situ* hybridization was carried out to characterize *STM* expression in the mutant SAM. Wild-type and *trn2*₃₀₁₀ plants were grown under long-day conditions, and 11-DAG-old seedlings and inflorescences were fixed and sectioned. The resulting serial sections were hybridized to an antisense *STM* probe. The data were collected from longitudinal sections because this allows the morphology of SAM to be easily observed.

During vegetative development, *STM* transcripts were detected in the SAM and excluded from leaf primordia in both *trn2*₃₀₁₀ and wild-type SAMs (Fig. 11A and C). The endogenous *STM* transcripts detected by the antisense probe in the whole enlarged mutant SAM suggested that the meristem identity of cells within the SAM was maintained, despite the changes in morphology. During the reproductive phase, RNA *in situ* hybridization revealed that *STM* transcripts are confined to the inflorescence and to the floral meristems of mutants, similar to wild-type plants (Fig. 11B and D). *STM* transcripts also accumulated in stem tissues of both wild-type and mutant plants and were therefore not uniquely restricted to the SAM (Long *et al.*, 1996). In mutant plants, the *STM* transcripts in stems were more strongly detected than that in the wild-type stem (Fig. 11B and D). This result may be an artifact due to the twisted architecture of the mutant stem, which means that sections maybe not in the compatible plane, as in the wild-type.

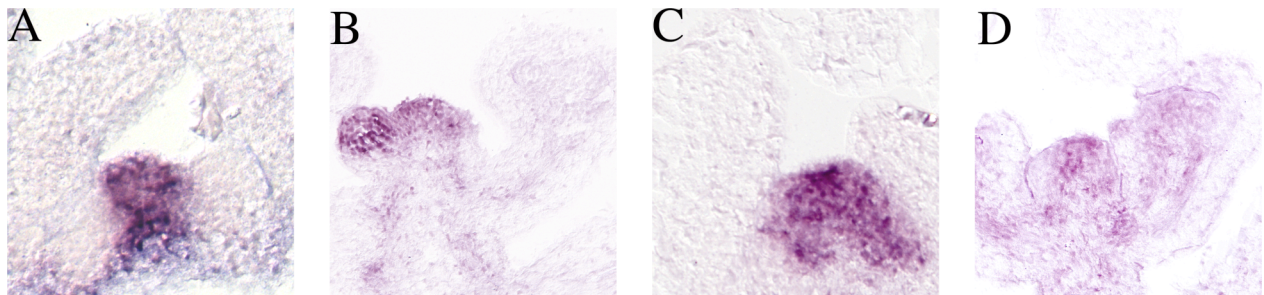


Figure 11. *STM* expression in wild-type and *trn2* meristems. (A) The longitudinal section of a 11-DAG-old wild-type seedling hybridized with the antisense *STM* probe shows that *STM* expression is confined to the SAM. *STM* transcripts are not detected in lateral organ primordia and leaves. (B) The longitudinal section of a wild-type inflorescence hybridized with the antisense *STM* probe revealed that *STM* transcripts accumulate in inflorescence and floral meristems, and also in stem tissues. (C) The

RESULTS

longitudinal section of a 11-DAG-old *trn2* seedling hybridized with the antisense *STM* probe. *STM* transcripts accumulate are confined in the aberrant SAM but not in organ primordia and leaves. **(D)** The longitudinal section of a *trn2* inflorescence hybridized with the antisense *STM* probe. *STM* transcripts accumulate in the inflorescence meristem in major like it accumulates in the wild-type inflorescence.

To summarize, in both wild-type and mutant plants, *STM* expression is confined in the vegetative SAM, inflorescence and floral meristems, and is downregulated in lateral organ primordia. Though the GUS activity was detected in mutant leaflets (Fig 2A), ectopic *STM* expressions in lateral organ primordia were not found by *in situ* hybridizations. No obvious evidences suggested that there is a significant change of the *STM* expression patterns in mutant plants; however, the endogenous *STM* transcripts accumulated in the enlarged mutant SAM suggests that the *STM* expression domain is increased.

3.5.3 *WUS* and *CLV3* expression patterns in *trn2* mutants

To gain a deeper insight into the organization of the *trn2* SAM, different meristem-related molecular markers were used in RNA *in situ* hybridization analysis. *WUS* and *CLV3* probes were used on 11-DAG-old *trn2* mutant and wild-type seedlings. These probes should indicate differences in the CZ relative to the surrounding PZ.

In the mutant SAM, *WUS* transcripts were detected in few cells in the L3 layer of the CZ, similar to what was observed in wild-type plants (Mayer *et al.*, 1998; Fig. 12A and B), suggesting that the expression pattern of *WUS* is not affected in the *trn2*₃₀₁₀ background. *CLV3* transcripts were detected in the same domain in *trn2* mutant SAM as in wild-type SAM (Fletcher *et al.*, 1999; Fig. 12C and D). However, the *CLV3* expression domain in the mutant SAM is relatively reduced compared with wild-type (Fig. 12C and D).

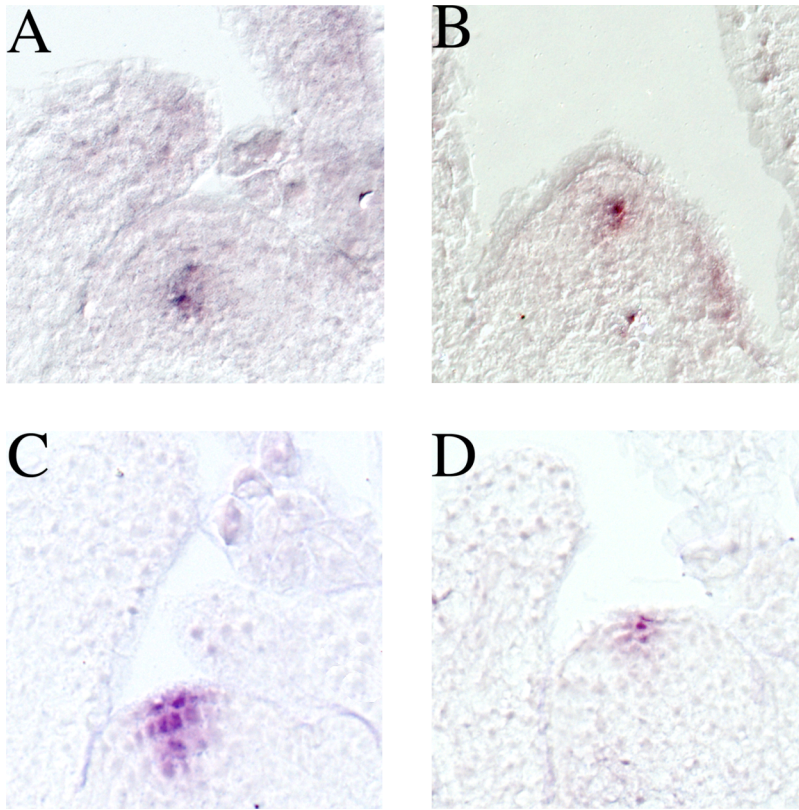


Figure 12. *WUS* and *CLV3* expression in the wild-type and *trn2* SAM. (A)(B) *WUS* expression in the wild-type and *trn2* SAM, respectively. (C)(D) *CLV3* expression in the wild-type and *trn2* SAM, respectively. Relative expression patterns of *WUS* and *CLV3* are not affected in the mutant SAM. However, the *CLV3* expression domain is reduced in the mutant SAM (D) compared with the wild-type (C).

Although the *trn2*₃₀₁₀ SAM has an aberrant morphology and is enlarged relative to wild-type, both molecular markers uncovered no major differences in the relative positions of the *CLV3* and *WUS* domains. The results suggested that the organization of the SAM is not affected in the *trn2* mutant. Both of these gene markers argue against the size of the stem-cell niche in the CZ being increased by the *trn2* mutation. Therefore, the enlargement and aberrant morphology of the mutant meristem must be the consequence of an increase in the PZ.

3.5.4 *LFY* expression in *trn2* mutants

11-DAG-old *trn2* plants have a protruding and enlarged SAM compared with wild-type. However, the earlier flowering time of *trn2* mutants argues that the change in SAM shape may relate to a switch from vegetative to reproductive phase. To exclude the possibility that the change in morphology in the mutant SAM is due to the floral transition, RNA *in situ* hybridization analysis was carried out using *LEAFY* (*LFY*) as a molecular marker for the reproductive phase.

The expression of *LFY* in the shoot tip is an early marker for the formation of flowers. The *LFY* gene encodes a plant-specific transcriptional factor. It is expressed in the newly emerging leaf primordia, but is absent from the SAM, and older leaves, during the vegetative phase. When the floral transition process begins, *LFY* is first expressed in subsets of cells in the PZ, presumably directing these cells toward a floral fate (Weigel *et al.*, 1992). Later, high levels of *LFY* transcripts are detected in flower primordia that have just formed (Blázquez *et al.*, 1997). Therefore, it is proposed that *LFY* is both necessary and sufficient for the initiation of individual flowers in the transition from the vegetative to the reproductive phase (Blázquez *et al.*, 1997).

As expected, in an 11-DAG-old wild-type plant (grown in long-day conditions), which was still at the vegetative phase, *LFY* transcripts could be detected only in newly emerged leaves but not in the SAM (Fig. 13A). Similar results were obtained from mutant seedlings. RNA *in situ* hybridizations revealed no detectable signals in the protruding SAM of *trn2* mutant plants, and no newly formed flower primordia were observed (Fig. 13B). These results suggested that the morphological changes in the 11-DAG-old mutant SAM were not related to the floral transition.

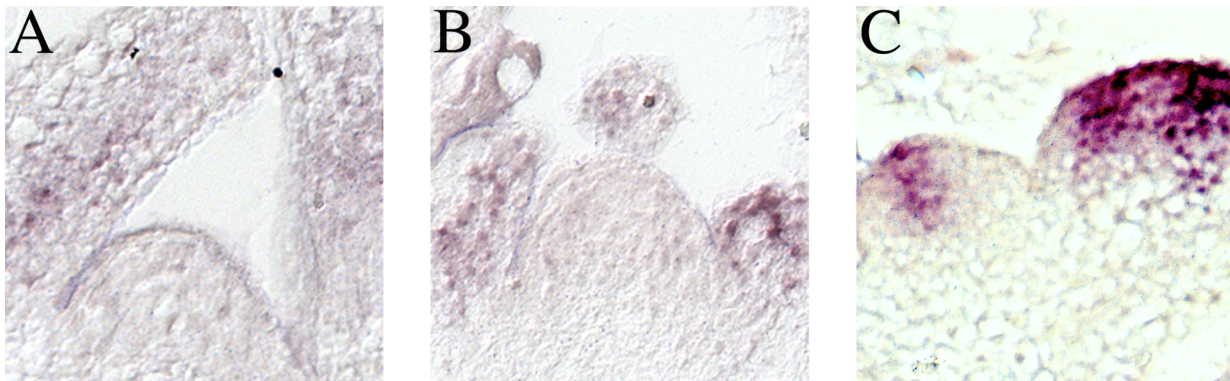


Figure 13. RNA *in situ* hybridization with the antisense *LFY* probe on the wild-type and the mutant SAM. (A) *LFY* transcripts were not detectable in the 11-DAG-old wild-type SAM, but signals were detected in young leaves. (B) In an 11-DAG-old *trn2₃₀₁₀* seedling, *LFY* transcripts were not detectable in the protruding SAM. As in the wild-type, *LFY* transcripts accumulated in young leaves. (C) A positive control of the *LFY* RNA *in situ* hybridization. In the inflorescence, the *LFY* transcripts accumulated in flower primordia and floral meristems.

3.6 Real-time RT-PCR experiments

In addition to gene expression patterns, it is interesting to consider whether the level of gene expression is affected in *trn2* plants. To answer this question, and to further understand meristem-related gene expression in mutant plants, real-time RT-PCR experiments were carried out to quantify the levels of *STM*, *WUS* and *CLV3* expression.

The real-time RT-PCR results are summarized in Table 2. The delta Ct values of *STM* gene of mutants were always lower than that of wild-type plants, and a Student's *t*-test gave *p* values less than 0.01. These results suggested that the amount of *STM* transcripts is significantly increased in *trn2* mutants. Using a previously described formula (Livak and Schmittgen, 2001) to calculate the relative amount of change of gene transcripts substantiated an, on average, 4.1-fold increase in *STM* transcripts in *trn2* seedlings relative to wild-type. For *WUS*, the delta Ct values were similar in both mutant and wild-type seedlings. The amount of *WUS* transcripts were increased, on average, 1.2-fold in mutant seedlings relative to wild-type. However, a Student's *t*-test showed *p* values larger than 0.05, suggesting that the increase is not significant. Therefore, it seems that *WUS* expression is not affected in *trn2* mutants. In contrast with *WUS*, the amount of *CLV3* transcripts was significantly affected in *trn2* mutants. The delta Ct values of *CLV3* in mutant seedlings were always higher than those of wild-type seedlings, indicating that there were fewer *CLV3* amplicons detected in real-time PCR reactions using the mutant cDNA as templates than using wild-type cDNA as templates. On average, *CLV3* transcripts were decreased 0.5-fold in mutant seedlings relative to wild-type. Moreover, a Student's *t*-test gave *p* values lower than 0.04, suggesting that the amount of *CLV3* transcripts decreases significantly in mutant seedlings.

Table 2. Gene expression changes in *trn2* plants

Gene name	Fold change ^a	P value ^b
<i>STM</i>	4.1 ± 2.5	<0.01
<i>WUS</i>	1.2 ± 0.1	>0.05
<i>CLV</i>	0.5 ± 0.1	<0.04

^aFold change, the mean of changes averaged from three independent real-time PCR reactions.

^bP value, generated by a t-test comparing Cts of the gene in wild-type and mutant plants. P value that is less than 0.05 suggests a significant difference.

Taken together these results indicate that, *trn2* mutants have increased levels of *STM* expression, similar levels of *WUS* and decreased levels of *CLV3* expression compared with wild-type. The increased *STM* transcripts in mutant seedlings are compatible with the observed *STM-GUS* pattern of expression, which suggested an increased *STM* domain. The decreased level of *CLV3* expression can be explained in several ways. *CLV3* RNA *in situ* hybridization analysis revealed a decreased *CLV3* expression domain, suggesting that there are fewer cells expressing *CLV3*. This is consistent with the result of real-time RT-PCR. A decrease in *CLV3* expression was expected to an increase of *WUS* expression. However, the results of RNA *in situ* hybridization and real-time RT-PCR revealed that *WUS* expression is not affected in *trn2* mutants.

3.7 Genetic interactions between *trn2* and other meristem-related genes

To further understand *TRN2* function, heterozygous *trn2*₃₀₁₀ plants were crossed with heterozygous *stm-1*, *stm-5* and *wus-1*, and homozygous *clv3-2* plants to create double mutants. Double mutants were then subjected to detailed phenotypic analysis to unravel the genetic interactions between *TRN2* and other meristem-related genes.

3.7.1 Genetic interactions between *trn2* and *stm*

3.7.1.1 *stm-5* and *stm-1* alleles and mutants

stm-5 contains a point mutation at the beginning of the second intron of *STM* gene. Mature *stm-5* embryos do not exhibit a recognizable SAM, and 7 days after germination *stm-5* young seedlings do not display leaves but the petioles of their cotyledons are partially fused. The production of other organs in *stm-5* plants is very delayed and they rarely have flowers (Endrizzi *et al.*, 1996).

stm-1 carries a nonsense mutation that encodes a protein missing the homeodomain. In homozygous *stm-1* embryos, no primary SAM is initiated, the mutant seedlings fail to produce any organs post-embryonically and they do not express *STM* (Long *et al.*, 1996).

3.7.1.2 Identification of double mutants for both *trn2* and *stm*

To isolate *trn2 stm* double mutants, 4-DAG-old F2 seedlings of *trn2₃₀₁₀* X *stm-1* or *stm-5* crosses without visible leaf primordia were picked out while wild-type seedlings developed visible leaf primordia. The no-leaves populations were supposed to be a mixture of single mutants and double mutants. To identify *stm-5 trn2₃₀₁₀* double mutants, statistical and genetic methods were used. A chi square test generated a value 3.11 (Table 3), suggesting that the segregation ratios are conformed to Mendelian rules. To characterize the genotype of the *stm-5 trn2₃₀₁₀* double mutants, DNA fragments containing the point mutation of *stm-5* and *trn2₃₀₁₀* were amplified from the genomic DNA of presumptive double mutants and the PCR products were then digested by *TaqI* to check *stm-5* and *EcoRI* to check *trn2₃₀₁₀* (Fig 14). The results revealed that those presumptive double mutants were homozygous of both *stm-5* and *trn2₃₀₁₀*. Based on the statistical test and the genotyping, *stm-5 trn2₃₀₁₀* double mutants were confirmed unambiguously.

Table 3. Results of chi square test

	Single			Double	chi square value	Null hypothesis ^d
	Wt ^a	Mutant ^b	<i>trn2₃₀₁₀</i> ^c	Mutant		
<i>trn2₃₀₁₀</i> X <i>stm-5</i> F2	658	203	225	54	3.11	Accepted

RESULTS

<i>trn2₃₀₁₀</i> X <i>stm-1</i> F2	132	32	36	9	4.56	Accepted
--	-----	----	----	---	------	----------

(Table 3. Continued)

<i>trn2₃₀₁₀</i> X <i>wus-1</i> F2	394	141	121	35	1.62	Accepted
<i>trn2₃₀₁₀</i> X <i>clv3-2</i> F2	404	143	150	42	0.73	Accepted
Expected ratio	9	3	3	1		

^aWt, including wild-type plants and heterozygotes of each mutant.

^bSingle mutant, homozygotes of *stm-5*, *stm-1*, *wus-1* or *clv3-2*.

^c*trn2₃₀₁₀*, homozygotes of *trn2₃₀₁₀*.

^dNull hypothesis, the null hypothesis is the expected ratio.

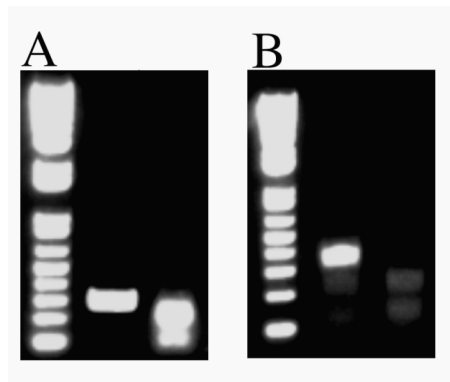


Figure 14. Check of *stm-5* and *trn2₃₀₁₀* fragments. (A) Intact *stm-5* fragment (left lane) and *stm-5* fragment digested by *Taq*I. (B) Intact *trn2₃₀₁₀* fragment (left lane) and *trn2₃₀₁₀* fragment digested by *Eco*RI.

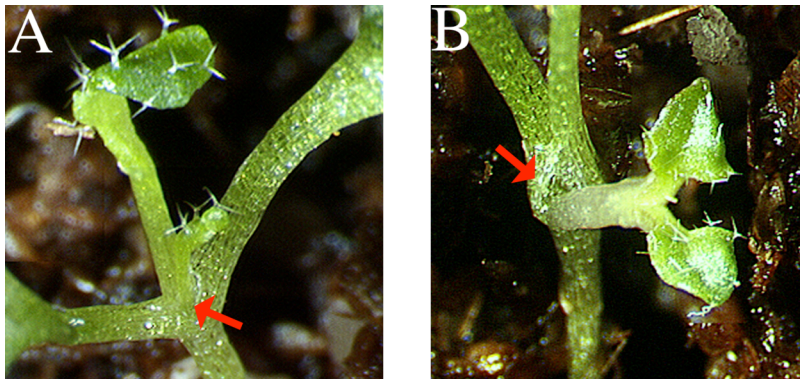
The same methods were also used to identify *stm-1 trn2₃₀₁₀* double mutants. Statistical tests indicated that one-in-sixteen plants in the population were presumptive double mutants (Table 3). DNA fragments carrying the point mutation of *stm-1* and *trn2₃₀₁₀* were amplified from the genomic DNA of presumptive double mutants by specifically designed primers. *trn2₃₀₁₀* fragments were checked by *Eco*RI digestion, and *stm-1* fragments were subjected to sequencing analysis (sequence data not shown). Taken together, the results of the statistical analysis and the genotyping unambiguously confirmed that *stm-1 trn2₃₀₁₀* double mutants were homozygous.

3.7.1.3 Phenotypic analyses of *trn2 stm* double mutants

In contrast with *stm-5* single mutants, in which only 3% plants developed leaves by 8 DAG (Table 4), 51.7% of *trn2₃₀₁₀ stm-5* double mutants developed at least one leaf before 8 DAG, and all double mutants developed leaves during a 20-day interval (Table 4). In addition to developing leaves more rapidly than the *stm-5* single mutant, only 20% of *trn2₃₀₁₀ stm-5* double mutants exhibited leaves with fused bases (Fig. 15A). During their lifetime, the *stm-5 trn2₃₀₁₀* double mutant plants continued to develop leaves from the shoot tip and bolting shoots and flowers were never observed.

A similar result was obtained from crosses of *trn2₃₀₁₀* and *stm-1*. 75.0% of *stm-1 trn2₃₀₁₀* double mutants began to develop leaves before 8 DAG and they all developed leaves by 20 days (Table 4), whereas *stm-1* plants did not develop leaves even one month after germination. However, *trn2₃₀₁₀ stm-1* leaves had fused petioles, which is a typical phenotype of *stm* mutants (Endrizzi *et al.*, 1996). In addition, 66% of double mutants developed leaves from the hypocotyl, implying the formation of an adventitious SAM (Fig. 15B). Furthermore, *trn2₃₀₁₀ stm-1* double mutants also developed leaves repetitively from the same site (shoot tips or the side of the hypocotyl) during their lifetime and bolting shoots and flowers were never observed.

Therefore, in both double mutant combinations, the *trn2₃₀₁₀* background can partially compensate for lost or reduced *STM* function. Unfortunately, none of the double mutant plantlets developed flowers which would have allowed phenotypic analysis during the reproductive phase.



RESULTS

Figure 15. Genetic interactions between *trn2* and *stm*. (A) The 11-DAG-old *trn2₃₀₁₀ stm-5* double mutant seedling. A pair of *trn2*-like leaves developing from the tip of the shoot (red arrow). Note that the bases of cotyledons and leaves are not fused whereas *stm-5* single mutants have leaves with fused petioles. (B) The 11-DAG-old *trn2₃₀₁₀ stm-1* double mutant seedling. The bases of cotyledons and leaves were always fused. Half of the double mutants developed leaves from the side of the hypocotyls (red arrow), suggesting the formation of an adventitious meristem.

Table 4. Genetic interactions between *trn2* and *stm*

Genotype	<i>n</i>	8 DAG ^a	No leaves ^b
<i>stm-1</i> (<i>Ler</i>) ^c	49	0.0%	100.0%
<i>stm-5</i> (<i>Ler</i>) ^c	29	3.0%	45.0%
<i>stm-1</i> (<i>Ler/Col</i>) ^d	38	5.3%	60.5%
<i>stm-5</i> (<i>Ler/Col</i>) ^d	38	24.2%	18.1%
<i>trn2₃₀₁₀ stm-1</i> (<i>Ler/Col</i>) ^d	40	75.0%	0.0%
<i>trn2₃₀₁₀ stm-5</i> (<i>Ler/Col</i>) ^d	54	51.7%	0.0%

^a8 DAG, the percentage of plants developing leaves 8 days after germination.

^bNo leaves, the percentage of plants did not develop leaves 20 days after germination.

^c(*Ler*), plants in the *Ler* background.

^d(*Ler/Col*), plants in the background of Col X *Ler*.

As *stm-1* and *stm-5* mutants are both in the Landsberg *erecta* background, whereas *trn2₃₀₁₀* mutants were created in the Columbia ecotype, the effect of timing to generate leaves may be a consequence of the cross of both ecotypes. To exclude this possibility, both *stm* alleles were back crossed to the Columbia background, and the time required for leaf generation in the F2 populations were examined.

Only 3% of *stm-5* single mutants (*Ler* background) developed leaves before 8 DAG. On the other hand, *stm-1* single mutants (*Ler* background) never developed leaves (Table 4). In populations of backcrosses, 24.2% of *stm-5* plants and 5.3% of *stm-1* plants began to develop leaves before 8

DAG. However, 18.1% of *stm-5* and 60.5% of *stm-1* plants did not develop leaves even after 20 DAG (Table 4). Although in the *Ler* X *Col* background both *stm-1* and *stm-5* mutant seedlings initiated leaves slightly more frequently than in the *Ler* ecotype, the difference was nowhere near as large as when combined with the *trn2₃₀₁₀* mutant background, where essentially all plants developed leaves 20 days after germination (Table 3). In conclusion, in both double mutant combinations, the *trn2* background can compensate for the reduced or lost *STM* activity and thus partially rescue the *stm* phenotype.

3.7.2 *trn2* and *wus*

3.7.2.1 The *wus-1* allele and mutant

wus-1 is a strong loss-of-function allele of *WUS* gene, which contains a point mutation in 5'-exon-intron boundary of intron 2 where the nucleotides were changed from GG to GA, replacing a G that is highly conserved at plant gene splice sites. The failure to remove intron 2 results in a translational stop after a few codons within the intron (Mayer et al., 1998). *wus-1* plants do not develop leaves 7 DAG while the wild-type shoot meristem gave rise to a rosette of leaves. After floral transition, to the inflorescence, *wus* mutants repetitively initiated defective shoot meristems, which give rise to only a few leaves and then discontinue primordia initiation. Eventually, disorganized bunches of leaves are observed at the base and the tip of several stems in mutants. Mutant flowers are rare and differed from wild-type in that they lack most central organs (carpels) and terminate most often in a single to few (but never six) central stamens (Laux et al., 1996) (Fig 16 C), and it was proposed that precocious consumption of the central region during definition of the third-whorl domain appears to be the basis of the *wus* floral phenotype (Laux et al., 1996).

3.7.2.2 Genetic interactions between *wus-1* and *trn2₃₀₁₀*

To identify *wus-1 trn2₃₀₁₀* double mutants, plants that did not develop leaves by 7 DAG were selected from the F2 population, and these presumptive double mutants developed twisted leaves several days later.

To confirm these presumptive double mutants, DNA sequence analyses and statistical methods

RESULTS

were used as described above. The calculated chi-squared value was 1.62, suggesting that the segregation ratio of the F2 population fitted the Mendelian ratio (Table 3). The genomic DNA of several presumptive double mutants was extracted, and the *trn2₃₀₁₀* fragment was amplified and checked. The *wus-1* fragment was also amplified by a specifically designed pair of primers and subjected to sequence analysis (sequence data not shown). Based on the phenotype, the statistical analysis and the genotype, these plants were confirmed to be homozygous for both *wus-1* and *trn2₃₀₁₀*.

During vegetative development, despite the dwarf stature and twisted organs of double mutants, the behavior of *wus-1* plants and double mutants was indistinguishable. The time for double mutants to develop leaves was as delayed as that of *wus-1* plants. After floral transition, a novel phenotype was observed in double mutant flowers. All *wus-1 trn2₃₀₁₀* flowers developed 2 carpels, whereas in *wus-1* mutants, carpels were completely absent (Fig. 16C) and only 1.6 stamens (compared with 6 in wild-type) developed in the third floral whorl (Table 5). Therefore, the *trn2* mutation may compensate for a premature consumption of stem cells in *wus-1* flowers, which is also consistent with the increased number of stamens (4.2 on average; Table 5) in the third floral whorl. In contrast, the number of sepals and petals in the outer two whorls was reduced and was closer in number in *trn2₃₀₁₀* than in *wus-1* single mutant flowers.

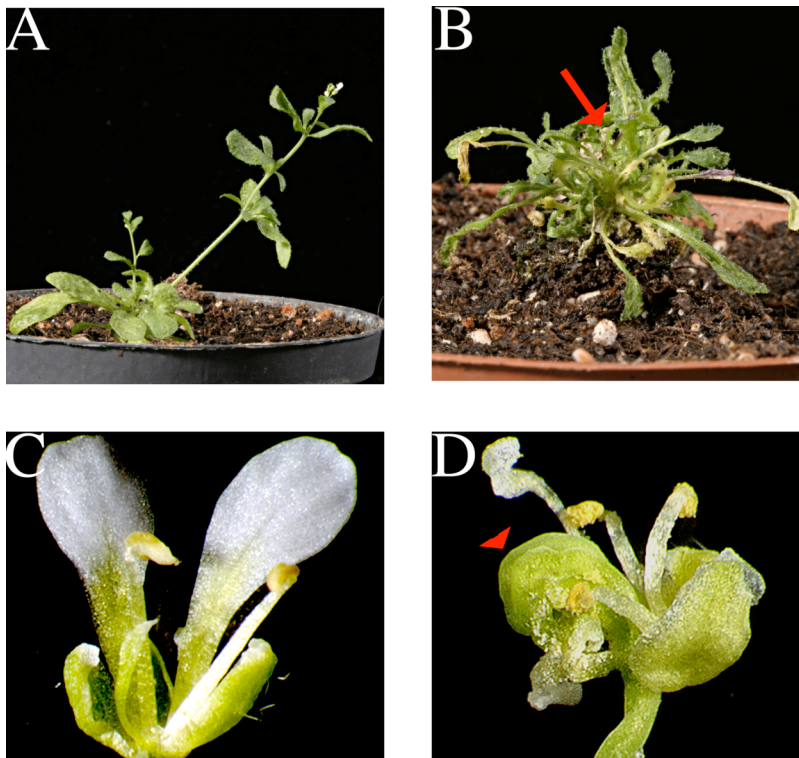


Figure 16. Genetic interactions between *trn2* and *wus*. (A) The one-month-old *wus-1* plant. (B) The one-month-old *trn2₃₀₁₀ wus-1* double mutant. The double mutant has dwarf stature like the *trn2* single mutant. The red arrow indicates flowers. (C) The *wus-1* flower. (D) The *trn2₃₀₁₀ wus-1* flower, which is like the *trn2₃₀₁₀* flower. Note that there is a severe twisted style with two unfused carpels at the floral center (red arrow head).

Table 5. The mean of floral organs

	Sepals	Petals	Stamens	Carpels	Carpels not fused
WT (n=31)	4.0 ± 0	4.0 ± 0	6.0 ± 0	2.0 ± 0	0.0%
<i>trn2₃₀₁₀</i> (n=39)	3.2 ± 0.8	2.4 ± 0.8	3.5 ± 1.0	2.0 ± 0	52.0%
<i>wus-1</i> (n=31)	3.7 ± 0.5	3.4 ± 1.0	1.6 ± 0.8	0.0	^a ND
<i>trn2₃₀₁₀ wus-1</i> (n=27)	3.2 ± 0.8	2.4 ± 1.1	4.2 ± 1.1	2.0 ± 0	33.0%

^aND, not detectable.

In conclusion, there was no additive phenotype observed in double mutants during the vegetative phase, but surprisingly, double mutant flowers were completely *trn2*-like. *wus-1* flowers lacked the most central organs, carpels, and generally had zero to three stamens, but the numbers of organs in the outer two whorls were on average only slightly reduced compared with wild-type (Table 5). In contrast, the double mutant flowers had fewer *trn2*-like organs in the outer three whorls compared with wild-type and two carpels at the center, which are never found in *wus-1* flowers, suggesting that the *trn2* background compensates for the prematured floral meristem of *wus-1* flowers. Furthermore, double mutants have typical twisted *trn2* lateral organs, suggesting that *TRN2* acts epistatically to *WUS*.

3.7.3 *trn2* and *clv3*

3.7.3.1 The *clv3-2* allele and mutant

clv3-2 was identified during a gamma-irradiation mutagenesis of Landsberg *erecta* seeds and

RESULTS

contained a deletion in the second intron of the gene. *clv3-2* plants have enlarged meristems throughout their lifetime. The enlarged inflorescence meristems of *clv3-2* result in thicker shoots compared with wild-type. The larger *clv3-2* floral meristem develops into a flower with additional organs in each whorl, and the number of stamens and carpels are more dramatically increased than petal and sepal number (Clark *et al.*, 1996).

3.7.3.2 Genetic interactions between *clv3-2* and *trn2₃₀₁₀*

It was difficult to identify *clv3-2 trn2₃₀₁₀* double mutants in the F₂ population on the basis of their phenotypes during the vegetative phase, suggesting that there was no additive phenotype for these double mutants. When flowering, some plants in the F₂ population were considered to be presumptive double mutants because of their twisted organs (typical of *trn2*) and thicker shoots (typical of *clv3*).

The same methods described above were used to confirm that these plants were homozygous for both *trn2₃₀₁₀* and *clv3-2*. The chi-squared test indicated that the segregation ratio fitted to the Mendelian ratio (Table 3). The *trn2₃₀₁₀* fragment was amplified and checked as described above, and the *clv3-2* fragment was amplified by a specifically designed pair primers and subjected to sequence analysis (sequence data not shown). The phenotype, the statistical test and the genotype together confirmed that these presumptive double mutants were homozygous for both *trn2₃₀₁₀* and *clv3-2*.

During the reproductive phase, an additional phenotype not observed in single *clv3-2* or *trn2₃₀₁₀* mutants was identified in double mutant flowers. Double mutant flowers had reduced organ numbers in the outer whorls of sepals, petals and stamens (Table 6), reminiscent of *trn2₃₀₁₀* single mutant flowers, and in contrast with *clv3-2* single mutant flowers (Fig. 17A), there was no increase in the number of stamens (Table 6). Also, when compared with the outer three whorls, there were supernumerary carpels at the floral center in double mutant flowers, as was observed in *clv3-2* flowers (Fig. 17B), and in 27% of double mutant flowers these carpels were unfused at their upper parts (Table 6). The reduced number of floral organs and the twisted morphology of double mutant flowers suggested that *TRN2* acts epistatically to *CLV3* in the outer three whorls. On the other hand, the supernumerary carpels and the increased percentage of carpel fusion may be due to prolonged *WUS* expression caused by the *clv3-2* background (see discussion).

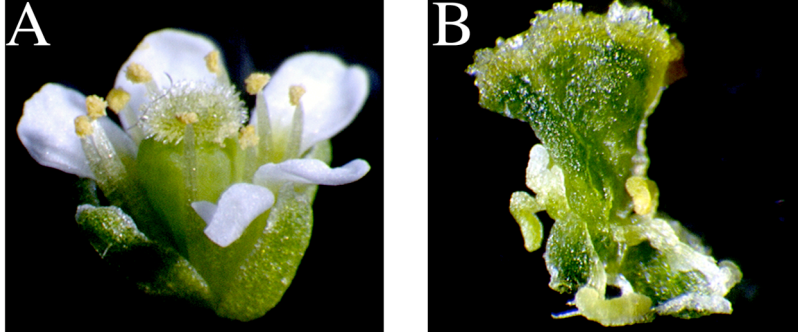


Figure 17. Genetic interactions between *trn2* and *clv3*. (A) The *clv3-2* flower. *clv3-2* flowers always have supernumerary floral organs. In this *clv3-2* flower, there are 5 sepals and petals, 8 stamens and a gynoecium within supernumerary carpels. (B) The *trn2₃₀₁₀clv3-2* flower. The flower has reduced number of floral organs in the outer three whorls (see table 5) but a gynoecium with supernumerary carpels fused together.

Table 6. The mean of floral organs

	Sepals	Petals	Stamens	Carpels	Carpels not fused
WT (n=31)	4.0 ± 0	4.0 ± 0	6.0 ± 0	2.0 ± 0	0.0%
<i>trn2₃₀₁₀</i> (n=39)	3.2 ± 0.8	2.4 ± 0.8	3.5 ± 1.0	2.0 ± 0	52.0%
<i>clv3-2</i> (n=34)	4.3 ± 0.4	4.1 ± 0.5	7 ± 0.9	^a Many	0.0%
<i>trn2₃₀₁₀clv3-2</i> (n=33)	2.1 ± 1	1.9 ± 1.1	2.8 ± 2.8	^a Many	27.0%

^aMany, multi-carpels-fused style.

4. DISCUSSION

4.1 The *TRN2* gene encodes a tetraspanin-like protein

Starting from a genetic screen designed to identify changes in *STM* promoter activity, a new *trn2* mutant allele was isolated, *trn2₃₀₁₀*. It carried the same G-A transition in the beginning of the second exon as the previously identified *trn2-2* allele (Cnops *et al.*, 2006). *trn2* mutants have dwarf stature, asymmetric leaves with aberrant vascular patterning and malformed inflorescences and flowers. The *TRN2* gene has been examined in many aspects, including root and leaf development (Cnops *et al.*, 2000; 2006); however, its role in the SAM has not been described. This study revealed that one of the peculiarities of *trn2* mutants is an aberrant SAM protruding and enlarged compared to wild-type, readily detected 11 DAG. The aberrant SAM morphology and malformed lateral organs suggest that the *TRN2* gene is implicated in SAM functions. In addition to careful inspection of the SAM histology, molecular markers were used to examine the change of gene expressions and the organization of the *trn2* SAM, and double mutants were also created to test genetic interactions between *trn2₃₀₁₀* and *stm-1*, *stm-5*, *clv3-2* and *wus-1*.

The *TRN2* gene encodes a protein of 269 amino acids that contains a tetraspanin domain at the N-terminal. Therefore, TRN2 can be considered as a plant tetraspanin protein. However, TRN2 protein contains a GCC motif in the LEL, instead of the conserved CCG motif that is characteristic of tetraspanin proteins, and in addition, TRN2 and its homologues among other plant species are grouped in one clade of a phylogenetic tree that is separate from the tetraspanins of animals, fungi, and amoeba (Huang *et al.*, 2005). Thus, TRN2 and its homologues are referred to as tetraspanin-like proteins.

Comparison of secondary structure between plant tetraspanin-like proteins and animal tetraspanin proteins revealed both groups of proteins were of similar size and shared the same topology, indicating that the plant tetraspanin-like proteins share structural homology with tetraspanin proteins (Cnops *et al.*, 2006). Specifically, the LEL found in animal tetraspanins seems to be relevant for complex formation with other proteins, as follows from genetic evidence and chimeric protein analysis (Hemler, 2001; 2003; Stipp *et al.*, 2003). Previous studies revealed that the homodimerization through LEL should be a basic unit in forming the TEM (Levy and Shoham, 2005; Hemler, 2005), and mutations in the LEL of tetraspanin CD151 disrupt direct

DISCUSSION

primary interaction with integrin and result in protein malfunction (Hemler, 2003). The point mutation in the *trn2₃₀₁₀* allele leading to a G to E amino acid exchange at position 81 in the LEL of the protein. Therefore, the amino acid exchange in the LEL of TRN2 might interfere the correct folding of the protein and interactions with associated proteins and disrupt the TRN2 normal function. Considering another previously identified allele, *trn2-1* (Cnops *et al.*, 2000), which lacks the entire LEL and has similar phenotype with *trn2₃₀₁₀*, LEL of TRN2 may play critical roles as of animal tetraspanin proteins.

Animal tetraspanins are found in nearly all tissue and cell types and they participate in divergent biological processes (Hemler, 2003). For example, CD81 is present in all types of cells within the immune system, has been implicated in both B cell and T cell immune responses and may serve as a receptor for HCV (Levy and Shoham 2005; McKeating *et al.*, 2004). *TRN2* is widely expressed in *Arabidopsis*, including in the SAM, in lateral organ primordia, in the incipient vasculature and in roots, suggesting that TRN2 tetraspanin-like proteins are involved in divergent biological processes in *Arabidopsis*, similar to the tetraspanin proteins in animals.

4.2 *trn2* mutation affects cell-fate decisions in the SAM

Previous studies (Cnops *et al.*, 2000) indicated that the radial patterning of the root meristem is incomplete in *trn2-2* mutant plants. Cell fates are inappropriately specified, with most irregularities seen in determined or differentiated cells such as the epidermal or lateral root-cap cell files. These data suggest that *TRN2* contributes to cell-fate decisions in the root meristem. The cotyledons of *trn2* plants develop relatively normal, but the lateral organs are twisted and malformed, arguing that the *trn2* phenotype may be due to a malfunction of the SAM. Twisted *trn2* rosette leaves usually rotate 180°; however, dorsolventrality of leaves is normal (Cnops *et al.*, 2006), suggesting that the *trn2* mutation does not affect the dorsal-ventral polarity of leaves. In contrast with dorsolventrality, *trn2* leaves are severely defective in symmetry and size. *trn2* leaves are smaller compared with wild-type and have asymmetric laminae, and the most conspicuous defect is the loss of half leaf blade. Furthermore, these defects are not restricted to the vegetative development; *trn2* flowers are small, asymmetric and have fewer floral organs in outer three whorls than wild-type. Both leaf lamina and floral organ missing may reflect that early steps of lateral organ anlagen development are disturbed in *trn2* mutants. *STM* RNA *in situ* hybridization revealed that the expression pattern of *STM* was confined to meristems in both

wild-type and *trn2* shoot tips. However, real-time RT-PCR experiments indicated that the amount of *STM* transcripts in *trn2* mutants is, on average, 4.1 times higher than in the wild-type, suggesting that excess *STM* transcripts accumulated in the *trn2* SAM. As *STM* maintains cells in an undifferentiated state (Long *et al.*, 2000), excess *STM* activity may inhibit cells from undergoing proper differentiation. Accordingly, the excess amount of *STM* transcripts detected in *trn2* seedlings suggests that cells in the PZ of the SAM, which should undergo differentiation in wild-type seedlings, cannot differentiate properly. Therefore, *TRN2* is required for proper cell differentiation in the SAM as well as in the root meristem. However, down-regulation of *STM* is still the earliest available signifier for the acquisition of the primordial fate (P₀) (Long *et al.*, 1996). In the absence of additional markers, it cannot be discriminated whether cells at the periphery of the *trn2* SAM are released for terminal differentiation in an appropriate timely or spatial fashion, or whether cells within the PZ of the SAM over-proliferate.

4.3 *TRN2* may contribute to another pathway rather than to *STM* pathway directly

To understand genetic interactions between *STM* and *TRN2*, heterozygotes of *trn2*₃₀₁₀ were crossed to heterozygous plants of *stm-1*, which is a null allele, and *stm-5*, which is a strong allele. Double mutant analyses revealed that *trn2* mutation promotes leaf development in either an *stm-1* or *stm-5* mutant background during early seedling development. It has been suggested that *stm-5* shoot meristems have cells that seem to prematurely undergo differentiation (these cells should remain undifferentiated in wild-type plants), and hence, the bases of the cotyledons and leaves of *stm-5* mutants are fused (Endrizzi *et al.*, 1996). However, not only do they form leaves more rapidly than *stm-5* single mutants, *trn2*₃₀₁₀ *stm-5* double mutants rarely have cotyledon and leaves with fused bases. The double mutant phenotype suggests a partial rescue of *stm-5* phenotype by *trn2*₃₀₁₀, and this rescue may arise from the accumulation of indeterminate cells at the shoot tip, which compensates for the premature *stm-5* meristem.

Similar results were obtained from *trn2*₃₀₁₀ *stm-1* double mutants. *stm-1* single mutants have cotyledons with fused bases and fail to form postembryonic organs because of the failure to establish a primary SAM during embryogenesis, whereas *trn2*₃₀₁₀ *stm-1* double mutants started to form leaves by 8 DAG. These results suggest that *trn2* mutation promote *stm-1* mutants to regain the meristematic activity. However, these double mutants always develop leaves with fused petioles. Therefore, the *stm-1* phenotype rescued by *trn2*₃₀₁₀ is not as complete as that observed

DISCUSSION

in *trn2₃₀₁₀ stm-5* double mutants with respect to fused organs. In addition, half of *trn2₃₀₁₀ stm-1* double mutants form adventitious meristems, suggesting that *trn2* may promote *stm-1* mutants to form a functional primary SAM during embryogenesis and to form meristems adventitiously while no functional primary SAMs are formed.

These results revealed that partial rescues of *stm* phenotype by the *trn2* mutation are not dependent on the strength of *stm* alleles with respect to the time to develop leaves, suggesting that the promotion of leaf development in the *trn2* background is not dependent on *stm* activity. Conversely, *stm* phenotype rescued by the *trn2* background is dependent on the strength of *stm* alleles with respect to organ fusion. Therefore, the *trn2* mutation may effect the contribution of meristem activity, independent of *STM* activity, to the promotion of leaf development. However, the effect of the *trn2* mutation is antagonistic to that caused by the *stm* mutation during the initiation of lateral organ primordia. These results suggest that *TRN2* may contribute to another pathway that crosslinks with the *STM* pathway.

Loss-of-function mutations in the *TRN1* locus result in similar phenotype to *trn2* mutants. It is predicted that the TRN1 is a large cytoplasmic protein that contains a putative LRR ribonuclease inhibitor-like (LRR-RI) subfamily domain at the N-terminal region (Cnops *et al.*, 2006). However, the kinase domain is absent. Other LRR proteins lacking kinase domains, such as CLV2, have been shown to be required for cellular communication processes that decide between stem-cell fate and a differentiated fate (Nadeau and Sack, 2003). Given that TRN2 is a tetraspanin-like protein, and may act in a similar manner to the animal tetraspanin proteins that are implicated in divergent signaling pathways (Hemler, 2003; 2005), and also recent studies that revealed that both *TRN1* and *TRN2* act in the same pathway (Cnops *et al.*, 2006), TRN1 is likely to be a component in the TRN2 pathway. The meristem phenotype and changes in gene expression caused by the *trn2* mutation suggest that the TRN2 pathway may contribute to normal meristem function. In addition, both *TRN2* and *TRN1* genes are conserved in angiosperm and gymnosperm (Cnops *et al.*, 2006), suggesting a presumptive signaling pathway established by the membrane bounded TRN2 protein and the cytoplasmic TRN1 protein is conserved during plant evolution.

4.4 *TRN2* affects auxin distribution and vasculature patterning in leaves

The dwarf stature and aberrant vascular patterning in leaves of *trn2* mutants are reminiscent of defects in auxin transport. Although the concentrations of endogenous IAA and the capacity to actively transport auxin were not altered in *trn2* plants, auxin distribution is severely altered in the leaves of *trn2* plants (Cnops *et al.*, 2006). Auxin distribution is correlated with the polar distribution of auxin efflux carrier PIN proteins and the direction of auxin transport can be monitored by the distribution of these proteins (Benková *et al.*, 2003; Friml *et al.*, 2003). PIN proteins are asymmetrically distributed in cellular membranes (Galweiler *et al.*, 1998), and in the SAM, the PIN1 protein is oriented toward those cells newly recruited for the P₀ primordia (Reinhardt *et al.*, 2003). Moreover, the basal localization of PIN1 is gradually established in the incipient vasculature below the primordia (Benková *et al.*, 2003). In this manner, auxin transport in the SAM and in the lateral organ primordia is dynamically directed towards new primordia and incipient vasculatures, respectively. However, how the orientations of PIN proteins are regulated is still unclear. TRN2 belongs to the tetraspanin-like family and may establish a tetraspanin-like protein enriched microdomain (TLEM) on the plasma membrane (similar to animal tetraspanin proteins) that then recruits associated proteins and facilitates their functions. In this way, TRN2 may contribute to the process of polar distribution of PIN proteins and affect the transport of auxin.

PIN1 also has a central role in mediating auxin distribution for patterning of phyllotaxis (Reinhardt *et al.*, 2003). However, phyllotactic patterns defects are not found in *trn2* plants, therefore TRN2 may not contribute a major role to auxin distribution in the SAM. In contrast, *TRN2* is preferentially expressed in the tips of leaflets — where the highest auxin concentration is detected during the leaf development (Mattsson *et al.*, 2003), and in the incipient midvein. Therefore, TRN2 may be implicated in the vascular patterning of leaves.

It was proposed that in both *as1* and *as2* mutants, the initial asymmetric placement of auxin at the leaf tip would give rise to later asymmetries in the internal auxin sources. This asymmetry would subsequently result in asymmetrical cell differentiation and division patterns (Zgurski *et al.*, 2005). *AS1* expression may be depressed due to the prolonged *STM* expression in *trn2* mutants during the initiation of lateral organ primordia. In this manner, loss of TRN2 activity may indirectly cause a decrease in *AS1* expression and subsequently cause the aberrant patterning of

the vasculature network. In compatible with this suggestion, it was reported recently that *TRN2* is synergistic with *AS1* with respect to venation patterning (Cnops *et al.*, 2006); and moreover, an altered auxin response pattern was observed in young leaflets of *trn2* mutants and *trn2* mutants also exhibited an ectopic and asymmetric distribution of auxin along the leaf margins of expanding leaves (Cnops *et al.*, 2006). These results suggest that *TRN2* is required for normal auxin distribution and vasculature patterning in leaves.

4.5 *trn2* mutation compensates meristem defects of *stm* and *wus* mutants

Double mutant analyses revealed that *trn2₃₀₁₀* partially rescues *stm* phenotype, suggesting that *trn2* mutation compensates for a loss-of-function SAM in *stm* mutants. Based on the *WUS* RNA *in situ* hybridization and real-time RT-PCR experiments, the expression domain of *WUS* and the amount of *WUS* transcripts are not affected in *trn2* mutants. These results suggest that the stem-cell organizing center is not altered in the mutant SAM. In contrast with *trn2₃₀₁₀stm* double mutants, combinations of both *trn2₃₀₁₀* and *wus-1* did not exhibit obviously additive phenotypes during the vegetative stage. Nevertheless, *trn2₃₀₁₀wus-1* flowers are *trn2*-like, and surprisingly, these double mutant flowers develop carpels at the floral center, which are lacking in *wus-1* single mutants (Laux *et al.*, 1996). Reminiscent of the enlarged SAM in the vegetative *trn2₃₀₁₀* seedling, the *trn2₃₀₁₀wus-1* double mutant floral meristem may contain an increased number of meristematic cells, which are not completely consumed through the precursor of outer whorl organs (as was the case in the *wus-1* single mutant; Laux *et al.*, 1996). If supernumerary meristem cells remain competent for the development of reproductive organs in the inner whorls, this could explain both the increase in stamen number and carpel development.

Taken together, these results indicate that *trn2* mutation promotes meristem activity and compensates for the *stm* and *wus* meristem phenotypes. Both the enlarged vegetative shoot apex and the partial rescue of the *stm* mutant phenotype in the *trn2₃₀₁₀* background suggest that *TRN2* may be involved in restricting meristem identity. This assumption is compatible with the lack of leaf segments observed (this study; Cnops *et al.*, 2006) when cells that are normally recruited as leaf founder cells (according to their position) are not released for primordial fate in a timely fashion. The twisted and malformed lateral organs of these double mutants suggest that *TRN2* acts epistatically to *STM* and *WUS*.

4.6 Genetic interactions between *trn2* and *clv3*

CLV3 RNA *in situ* hybridizations revealed that the *CLV3* expression domain is decreased in *trn2* seedlings and real-time RT-PCR experiments indicated that the amount of *CLV3* transcripts is half of the wild-type. Therefore, it is suggested that *CLV3* expression is decreased in *trn2* mutants. However, an expanded OC would be expected on a background of decreased *CLV3* expression, yet this is not observed in *trn2* mutants. A possible explanation is that although *CLV3* expression is decreased, the amount of the gene product, the CLV3 peptide ligand, is still above the threshold required to maintain the homeostasis of the OC. A Student's *t*-test gave a *p* value of less than 0.04 on average, suggesting a significant difference in the amount of *CLV3* transcripts between *trn2* mutants and wild-type plants. However, the decrease in *CLV3* transcripts in *trn2* seedlings is not as marked as the increase of *STM* transcripts (Table 2). Nevertheless, the possibility that *TRN2* participates in the regulation of *CLV3* expression cannot be unambiguously excluded.

Double mutant analyses revealed that no additive phenotype was observed in the *trn2₃₀₁₀ clv3-2* double mutants during vegetative development. Conversely, during reproductive development, *trn2₃₀₁₀* was epistatic to *clv3-2* and organ numbers in the three outer whorls of sepals, petals and stamens resembled those observed in *trn2₃₀₁₀* mutant flowers, and not the increased numbers observed in *clv3-2* flowers. In addition, instead of 2 mostly unfused carpels in *trn2₃₀₁₀* single mutants, the *trn2₃₀₁₀ clv3-2* double mutant flowers all contained supernumerary carpels, which were generally fused (>70%) to a single twisted style. Consequently, double mutant flowers of *trn2₃₀₁₀ clv3-2* plants showed *trn2₃₀₁₀*-specific reductions in organ number in the outer whorls of sepals and petals, and even decreased stamen number relative to *clv3-2* alone, whereas additional organs were formed in the inner carpel whorl in double mutant combinations.

Supernumerary carpels at the center of *trn2₃₀₁₀ clv3-2* flowers suggest that *clv3-2* phenotype is not rescued by the *trn2* background in the innermost whorl of the flower, and this is reminiscent of the phenotype of prolonged *WUS*-expressing flowers (Lenhard *et al.*, 2001). The activity of stem cells in the floral meristem has to be terminated after all organ primordia are formed, otherwise more than four whorls will be formed in *Arabidopsis* flowers. *WUS* expression is discontinued after stage 6 when carpel primordia are initiated (Mayer *et al.*, 1998; Lenhard *et al.*, 2001). Prolonged *WUS* expression in whorl 4, in a wild-type background, was shown to be

sufficient for floral meristem indeterminacy and resulted in massively proliferated gynoecium (Lenhard *et al.*, 2001). *AGAMOUS* (*AG*) is a direct target of *WUS* and it was shown to be an inhibitor of *WUS* expression, thus creating a negative feedback to *WUS* in the floral meristem (Lenhard *et al.*, 2001; Lohmann *et al.*, 2001). However, *AG* alone is not sufficient to terminate *WUS* expression completely (Mizukami and Ma, 1997). *WUS* expression is more strongly increased in *ag-1 clv1-4* double mutants compared with *ag-1* single mutants (Lohman *et al.*, 2001). Components of the *CLV* pathway, therefore, are candidates for cooperation with *AG* to terminate *WUS* expression (Schoof *et al.*, 2000). Thus, in *trn2* mutants, *CLV* and *AG* pathways are both active and *WUS* expression can be properly terminated after the formation of carpel primordia. However, in the *trn2₃₀₁₀ clv3-2* background, *CLV3* activity is depleted and only the *AG* pathway is active. *WUS* expression is therefore prolonged in floral meristems and causes supernumerary carpels at the flower center.

4.7 *TRN2* contributes to maintain a normal meristem function

A peculiarity of *trn2* mutants is an enlargement of the shoot apex, which is readily detectable in the *STM:GUS* background at 11 DAG. However, floral buds are not observed at this stage and the expression of the gene *LFY*, a molecular marker for floral transition, was not detectable by RNA *in situ* hybridization in the *trn2* SAM as in the wild-type SAM. This result indicates that the morphology change of the mutant SAM is not related to the floral transition. In addition, the discrepancy between the wild-type and *trn2* SAM is not evident before 7 DAG, suggesting that the enlargement of the *trn2* SAM is progressively accumulated during development. Based on RNA *in situ* hybridizations, *WUS* and *CLV3* expression domains are not increased relative to the enlarged SAM, indicating that the stem-cell niche in the CZ is not increased in the mutant SAM. Therefore, an enlargement of the PZ could account for the enlarged SAM.

Genetic analyses of double mutants of *trn2₃₀₁₀* and *stm* or *wus-1* indicated that mutation of *trn2* may promote meristem activity. The progressively increased size, and the final aberrant morphology, of the *trn2* SAM may reflect the gradual accumulation of indeterminate cells in the PZ. Excess number of indeterminate cells in the PZ may be the consequence of increased cell division rates in the CZ, which serves as a reservoir for stem cells and the PZ, or the proper recruitment of the cells in the PZ by lateral organ primordia is inhibited, or both. Increased rates of cell division in the CZ may cause an expansion of the CZ. However, this was not observed

DISCUSSION

when the stem-cell marker, *CLV3*, was used. Conversely, the *trn2* phenotype of delayed leaf initiation, lamina missing in leaves and fewer floral organs implies that this mutation causes defects in the early steps of lateral organ primordia development. Moreover, these defects are reminiscent of *mgoun1* (*mgo1*) and *mgo2* mutant phenotypes. Both *mgo1* and *mgo2* plants have an enlarged SAM, which progressively enlarges between 8 and 12 days (Laufs *et al.*, 1998a), and are defective in delayed leaf initiation compared with wild-type (Laufs *et al.*, 1998a), have asymmetric leaves and flowers that are missing organs (Laufs *et al.*, 1998a). These defects are the consequences of perturbation in initiation of primordia at the meristem periphery and the meristem outgrowth in *mgo* mutants may be a secondary effect of the perturbed primordia formation — instead of cells being recruited by the primordia they remain in the PZ (Laufs *et al.*, 1998a; 1998b). In addition, although the *trn2* SAM is larger than wild-type SAM, the vegetative meristem produces fewer leaves compared with wild-type, despite the fact that there are enough cells. *trn2* mutants are different from mutants that perturb the stem cell niche (such as *clv* or *wus*), where the number of organs is positively correlated with the number of cells produced by the meristem. Taken together, these data strongly suggest that cells in the PZ of the SAM are not properly recruited by lateral organ primordia in *trn2* mutants. Instead, they are maintained in an indeterminate state and remain in the PZ.

Excess accumulation of indeterminate cells in the PZ may be related to the higher activity of *STM*, suggesting that excess *STM* activity in *trn2* mutants disturbs normal meristem function — even it is not ectopically expressed in lateral organ primordia. Double mutant analyses revealed that meristem activity in *stm-1* mutants is recovered in a *trn2* background, suggesting that the major function of the wild-type *TRN2* gene is to limit the meristem identity. Considering that both *TRN2* and *STM* are expressed in overlapping patterns in the SAM, and that *TRN2* may act in another pathway rather than *STM* pathway, it is therefore suggested that *TRN2* may contribute to maintain a normal function of the SAM by regulating *STM* activity, either directly or indirectly.

In conclusion, an EMS mutagenesis effector screen performed with the *STM:GUS* marker line in *Arabidopsis thaliana* identified the *trn2₃₀₁₀* allele. The lesion in *trn2₃₀₁₀* was identical to that in the *trn2-2* allele, which carries a single G to A transition in the coding region of the second extra cellular loop of the *TRN2* tetraspanin protein. Histological and genetic analyses described here implicate *TRN2* in SAM function, as the peripheral zone appears enlarged relative to the central stem-cell zone in *trn2* mutants. The *trn2₃₀₁₀* allele can partially rescue *stm* mutant phenotypes

DISCUSSION

during seedling development, but is epistatic to *wus-1* and *clv3-2* alleles during the vegetative phase and in the outer floral whorls. The development of carpels in *trn2₃₀₁₀ wus-1* flowers suggests that pluripotent cells persist, in absence of the *TRN2* function, to the end of floral development. These data indicate a role for a membrane bound plant tetraspanin-like protein meristem function.

5. SUMMARY

(In English)

The aerial part of higher plants is derived from the SAM. In *Arabidopsis thaliana*, *STM* is the gene required to initiate and maintain the meristem. To understand how *STM* is regulated during developmental processes, an EMS-mutagenesis screen was carried out to isolate the gene(s) that affects *STM* expression. A line containing a quarter of plants with expanded GUS activity in shoot tips was isolated, and based on the genetic mapping, the mutant locus was confirmed to be allelic to *tornado2* (*trn2*). Previous studies (Cnops, et al., 2000; Olmos et al., 2003) showed that *TRN2* gene encodes a tetraspanin-like protein and its mutation causes dwarf plants, twisted lateral organs and inflorescence shoots, and abnormal development of roots. However, its functions in the SAM have not been described. In this study, it was showed that *trn2* mutants have an enlarged SAM within excess *STM* transcripts. *TRN2* is expressed not only in all types of meristems, which overlaps with *STM* expression patterns, but also in lateral organ primordia and in incipient vascular tissues. This expression pattern of *TRN2* is compatible with the higher accumulation of *STM* transcripts in mutants and the pleiotropic phenotype of *trn2* plants. Besides, *WUS* expression is not affected whereas the amount of *CLV3* transcript is decreased in mutants. Genetic interactions showed that *trn2* partially rescued *stm* phenotype and acts epistatically to *wus* and *clv3*, though there was no additive phenotype found in *trn2* and *wus* or *clv3* double mutants during the vegetative phase, *trn2* mutation restored the carpels development in *wus-1* background and made flowers to become *trn2*-like but still have supernumerary carpels in the *clv3-2* background. Since the central zone (CZ) is not increased relative to the enlarged SAM, the increase of the periphery zone (PZ) could account for the enlargement of the SAM. Taken together, these results suggest that *TRN2* functions in limiting the meristem activity, and loss of function of *TRN2* protein causes more cells undifferentiated and increases the meristematic activity.

6. ZUSAMMENFASSUNG

(Auf Deutsch)

Oberirdische Pflanzenteile entstammen dem Sproßapikalmeristem (SAM). In *Arabidopsis thaliana* ist *STM* das Gen, das benötigt wird, um das Meristem zu initiieren und aufrechtzuerhalten. Um zu verstehen, wie *STM* während des Entwicklungsprozesses reguliert wird, wurde ein EMS-Mutagenese-Screen durchgeführt, um auf diese Weise Gene zu isolieren, die die *STM*-Expression beeinflussen. Dabei wurde eine Linie gefunden, in der ein Viertel der Pflanzen verstärkte GUS-Aktivität in den Sproßspitzen zeigten. Mit Hilfe von Gen-mapping konnte gezeigt werden, dass die Mutation allelisch zu *tornado2* (*trn2*) ist. Vorangehende Studien (Cnops, et al., 2000; Olmos et al., 2003) haben gezeigt, dass *TRN2* für ein Tetraspanin-ähnliches Protein kodiert. Mutationen rufen verkümmertes Pflanzen mit verdrehten lateralen Organen und Infloreszenzsprossen sowie abnormale Wurzelentwicklung hervor. Allerdings wurde bisher die Funktion im SAM nicht beschrieben.

In dieser Arbeit konnte gezeigt werden, dass *trn2* Mutanten ein vergrößertes SAM mit einem Überschuss an *STM* ausbilden. *TRN2* wird nicht nur in allen Arten von Meristemen überlappend zum *STM*-Expressionsmuster angeschaltet, sondern zusätzlich in den Primordien der lateralen Organe und in sich entwickelndem vaskulärem Gewebe.

Dieses Expressionsmuster von *TRN2* ist kompatibel zu der stärkeren Anhäufung des *STM*-Transkripts in Mutanten und dem pleiotropen Phänotyp der *trn2*-Pflanzen. Zusätzlich konnte gezeigt werden, dass die *WUS*-Expression nicht beeinflusst wird, während die Menge des *CLV3* Transkripts reduziert ist. Genetische Interaktionen zeigen, dass *trn2* teilweise den *stm* Phänotyp retten kann und epistatisch zu *wus* und *clv3* wirkt. Obwohl kein zusätzlicher Phänotyp während der vegetativen Phase in *trn2 wus* oder *trn2 clv3* Doppelmutanten gefunden wurde, konnte *trn2* die Entwicklung der Fruchtblätter im *wus-1* Hintergrund wiederherstellen und führte zu Blüten ähnlich denen in *trn2*-Singlemutanten, im *clv3-2* Hintergrund blieb allerdings die Anzahl der Karpellen erhöht. Da die zentrale Zone (CZ) relativ zum vergrößerten SAM nicht zunimmt, ist anzunehmen, dass die Ausdehnung des SAM mit der Vergrößerung der peripheren Zone (PZ) zusammenhängt.

ZUSAMMENFASSUNG

Zusammenfassend lässt sich aus diesen Ergebnissen schließen, dass *TRN2* bei der Begrenzung der Meristemidentität mitwirkt und ein Verlust des TRN2 Proteins zur Folge hat, dass die Anzahl der undifferenzierten Zellen erhöht wird und somit die Region meristematischer Aktivität vergrößert wird.

7. BIBLIOGRAPHY

Ausubel, F. (Hrsg. 1996) Current protocols in molecular biology. *John Wiley & Sons, New York.*

Barton MK, and Poethig RS. (1993) Formation of the shoot apical meristem in *Arabidopsis thaliana*: an analysis of development in the wild-type and in the *shoot meristemless* mutant. *Development* 119, 823-831.

Barton MK. (2001) Leaving the meristem behind: regulation of *KNOX* genes. *Genome Biol.* 2(1): reviews 1002.

Bellaoui M, Pidkowich MS, Samach A, Kushalappa K, Kohalmi SE, Modrusan Z, Crosby WL, Haughn GW. (2001) The Arabidopsis BELL1 and KNOX TALE homeodomain proteins interact through a domain conserved between plants and animals. *Plant Cell.* 13(11), 2455-70.

Benková E, Michniewicz M, Sauer M, Teichmann T, Seifertova D, Jurgens G, Friml J. (2003) Local, efflux-dependent auxin gradients as a common module for plant organ formation. *Cell.* 115(5), 591-602.

Blázquez MA, Soowal LN, Lee I, Weigel D. (1997) *LEAFY* expression and flower initiation in Arabidopsis. *Development* 124(19), 3835-44.

Bowman JL, and Eshed Y. (2000). Formation and maintenance of the shoot apical meristem. *Trends Plant Sci.* 5, 110-115.

Bradley D, Carpenter R, Sommer H, Hartley N, Coen E. (1993) Complementary floral homeotic phenotypes result from opposite orientations of a transposon at the *plena* locus of *Antirrhinum*. *Cell.* 72(1), 85-95.

Brand U, Fletcher JC, Hobe M, Meyerowitz EM and Simon R. (2000) Dependence of stem cell fate in *Arabidopsis* on a feedback loop regulated by *CLV3* activity. *Science* 289, 617-619.

BIBLIOGRAPHY

Brand U, Hobe M and Simon R. (2001) Functional domains in plant shoot meristems. *Bioessays*. 23(2), 134-41.

Brand U, Grunewald M, Hobe M, Simon R. (2002) Regulation of CLV3 expression by two homeobox genes in Arabidopsis. *Plant Physiol*. 129, 565–575.

Byrne ME, Barley R, Curtis M, Arroyo JM, Dunham M, Hudson A and Martienssen RA. (2000) *Asymmetric leaves1* mediates leaf patterning and stem cell function in *Arabidopsis*. *Nature* 408, 967-970.

Carles CC and Fletcher JC. (2003) Shoot apical meristem maintenance: the art of a dynamic balance. *Trends Plant Sci*. 8(8), 394-401.

Carlioni V, Mazzocca A, Ravichandran KS. (2004) Tetraspanin CD81 is linked to ERK/MAPKinase signaling by Shc in liver tumor cells. *Oncogene*. 23(8), 1566-74.

Chen X, Zehnbauser B, Gnirke A, Kwok PY. (1997) Fluorescence energy transfer detection as a homogeneous DNA diagnostic method. *Proc Natl Acad Sci U S A*. 94(20), 10756-61.

Chuck G, Lincoln C, Hake S. (1996) KNAT1 induces lobed leaves with ectopic meristems when overexpressed in *Arabidopsis*. *Plant Cell* (8), 1277-89.

Clark SE, Runing MP and Meyerowitz EM. (1993) *CLAVATA1*, a regulator of meristem and flower development in *Arabidopsis*. *Development* 119, 397-418.

Clark SE, Jacobsen SE, Levin JZ and Meyerowitz EM. (1996) The *CLAVATA* and *SHOOT MERISTEMLESS* loci competitively regulate meristem activity in *Arabidopsis*. *Development* 122, 1567-1575.

Clark SE, Williams RW and Meyerowitz EM. (1997) The *CLAVATA1* gene encodes a putative receptor kinase that controls shoot and floral meristem size in *Arabidopsis*. *Cell* 89, 575-585.

BIBLIOGRAPHY

Clergeot PH, Gourgues M, Cots J, Laurans F, Latorse MP, Pepin R, Tharreau D, Notteghem JL, Lebrun MH. (2001) PLS1, a gene encoding a tetraspanin-like protein, is required for penetration of rice leaf by the fungal pathogen *Magnaporthe grisea*. *Proc Natl Acad Sci U S A.* 98(12), 6963-8.

Cnops G, den Boer B, Gerats A, Van Montagu M, Van Lijsebettens M. (1996) Chromosome landing at the *Arabidopsis TORNADO1* locus using an AFLP-based strategy. *Mol Gen Genet.* 253(1-2), 32-41.

Cnops G, Wang X, Linstead P, Montagu MV, Lijsebettens MV and Dolan L. (2000) *TORNADO1* and *TORNADO2* are required for the specification of radial and circumferential pattern in the *Arabidopsis* root. *Development* 127, 3385-3394.

Cnops G, Neyt P, Raes J, Petrarulo M, Nelissen H, Malenica N, Luschnig C, Tietz O, Dittengou F, Palme K, Azmi A, Prinsen E and Lijsebettens MV. (2006) The *TORNADO1* and *TORNADO2* genes have a function in several patterning processes during early leaf development in *Arabidopsis thaliana*. *Plant Cell.* 18(4), 852-66.

Cole M, Nolte C, Werr W. (2006) Nuclear import of the transcription factor SHOOT MERISTEMLESS depends on heterodimerization with BLH proteins expressed in discrete sub-domains of the shoot apical meristem of *Arabidopsis thaliana*. *Nucleic Acids Res.* 34(4), 1281-92.

Dheda K, Huggett JF, Bustin SA, Johnson MA, Rook G, Zumla A. (2004) Validation of housekeeping genes for normalizing RNA expression in real-time PCR. *Biotechniques.* 37(1), 112-4, 116, 118-9.

Doerner P. (2003) Plant meristems: a merry-go-round of signals. *Curr Biol.* 13(9), R368-74.

Endrizzi K, Moussian B, Haecker A, Levin JZ and Laux T. (1996) The *SHOOT MERISTEMLESS* gene is required for maintenance of undifferentiated cells in *Arabidopsis* shoot and floral meristems and acts at a different regulatory level than the meristem genes *WUSCHEL* and *ZWILLE*. *The Plant Journal* 10 (6), 967-979.

BIBLIOGRAPHY

Friml J. (2003) Auxin transport - shaping the plant. *Curr Opin Plant Biol.* 6(1), 7-12.

Friml J, Vieten A, Sauer M, Weijers D, Schwarz H, Hamann T, Offringa R, Jurgens G. (2003) Efflux-dependent auxin gradients establish the apical-basal axis of Arabidopsis. *Nature.* 426(6963), 147-53.

Fletcher JC, Brand U, Running MP, Simon R and Meyerowitz EM. (1999) Signaling of cell fate decisions by *CLAVATA3* in *Arabidopsis* shoot meristems. *Science* 283, 1911-1914.

Galweiler L, Guan C, Muller A, Wisman E, Mendgen K, Yephremov A, Palme K. (1998) Regulation of polar auxin transport by AtPIN1 in *Arabidopsis* vascular tissue. *Science.* 282(5397), 2226-30.

Gourgues M, Brunet-Simon A, Lebrun MH, Levis C. (2004) The tetraspanin BcPls1 is required for appressorium-mediated penetration of *Botrytis cinerea* into host plant leaves. *Mol Microbiol.* 51(3), 619-29.

Hake S, Smith HM, Holtan H, Magnani E, Mele G, Ramirez J. (2004) The role of knox genes in plant development. *Annu Rev Cell Dev Biol.* 20, 125-51.

Hay A, Kaur H, Phillips A, Hedden P, Hake S, Tsiantis M. (2002) The gibberellin pathway mediates KNOTTED1-type homeobox function in plants with different body plans. *Curr Biol.* 12(18), 1557-65.

Hemler ME. (2001) Specific tetraspanin functions. *J Cell Biol.* 155(7),1103-7

Hemler ME. (2003) Tetraspanin proteins mediate cellular penetration, invasion, and fusion events and define a novel type of membrane microdomain. *Annu Rev Cell Dev Biol.* 19, 397-422.

Hemler ME. (2005) Tetraspanin functions and associated microdomains. *Nat Rev Mol Cell Biol.* 6(10), 801-11

BIBLIOGRAPHY

Hiyoshi M, Hosoi S. (1994) Assay of DNA denaturation by polymerase chain reaction-driven fluorescent label incorporation and fluorescence resonance energy transfer. *Anal Biochem.* 221(2), 306-11.

Holland PM, Abramson RD, Watson R, Gelfand DH. (1991) Detection of specific polymerase chain reaction product by utilizing the 5'----3' exonuclease activity of *Thermus aquaticus* DNA polymerase. *Proc Natl Acad Sci U S A.* 88(16), 7276-80.

Huang S, Yuan S, Dong M, Su J, Yu C, Shen Y, Xie X, Yu Y, Yu X, Chen S, Zhang S, Pontarotti P, Xu A. (2005) The phylogenetic analysis of tetraspanins projects the evolution of cell-cell interactions from unicellular to multicellular organisms. *Genomics.* 86(6), 674-84.

Jasinski S, Piazza P, Craft J, Hay A, Woolley L, Rieu I, Phillips A, Hedden P, Tsiantis M. (2005) KNOX action in *Arabidopsis* is mediated by coordinate regulation of cytokinin and gibberellin activities. *Curr Biol.* 15(17), 1560-5.

Jeong S, Trotochaud AE and Clare SE. (1999) The *Arabidopsis CLAVATA2* gene encodes a receptor-like protein required for the stability of the CLAVATA1 receptor-like kinase. *The plant cell* 11, 1925-1933.

Kerstetter RA, Laudencia-Chinguanco D, Smith LG, Hake S. (1997) Loss-of-function mutations in the maize homeobox gene, *knotted1*, are defective in shoot meristem maintenance. *Development.* 124(16), 3045-54.

Kirch T, Simon R, Grunewald M and Werr W. (2003) The *DORNROSCHEN/ENHANCER OF SHOOT REGENERATION1* gene of *Arabidopsis* acts in the control of meristem cell fate and lateral organ development. *Plant Cell* 15, 694-705.

Konieczny A, Ausubel FM. (1993) A procedure for mapping *Arabidopsis* mutations using co-dominant ecotype-specific PCR-based markers. *Plant J.* 4(2), 403-10.

Kopczynski CC, Davis GW, Goodman CS. (1996) A neural tetraspanin, encoded by late bloomer, that facilitates synapse formation. *Science.* 1996 271(5257), 1867-70.

BIBLIOGRAPHY

Laufs P, Dockx J, Kronenberger J, Traas J. (1998) MGOUN1 and MGOUN2: two genes required for primordium initiation at the shoot apical and floral meristems in *Arabidopsis thaliana*. *Development*. 125(7), 1253-60.

Laux T, Mayer KF, Berger J, Jurgens G. (1996) The WUSCHEL gene is required for shoot and floral meristem integrity in *Arabidopsis*. *Development*. 122(1), 87-96.

Levy S, Shoham T. (2005) The tetraspanin web modulates immune-signalling complexes. *Nat Rev Immunol*. 5(2), 136-48.

Lincoln C, Long J, Yamaguchi J, Serikawa K, Hake S. (1994) A knotted1-like homeobox gene in *Arabidopsis* is expressed in the vegetative meristem and dramatically alters leaf morphology when overexpressed in transgenic plants. *Plant Cell*. 6(12), 1859-1876.

Livak KJ, Schmittgen TD. (2001) Analysis of relative gene expression data using real-time quantitative PCR and the $2^{-\Delta\Delta C(T)}$ Method. *Methods*. 25(4), 402-8.

Long JA, Moan EI, Medford JI and Barton MK. (1996) A member of the KNOTTED class of homeodomain proteins encoded by the *STM* gene of *Arabidopsis*. *Nature* 379, 66-69.

Long JA, Barton MK. (1998) The development of apical embryonic pattern in *Arabidopsis*. *Development*. 125(16), 3027-35.

Long J and Barton MK. (2000) Initiation of axillary and floral meristems in *Arabidopsis*. *Developmental Biology* 218(2), 341-353.

Mattsson J, Ckurshumova W, Berleth T. (2003) Auxin signaling in *Arabidopsis* leaf vascular development. *Plant Physiol*. 131(3), 1327-39.

Mayer KF, Schoof H, Haecker A, Lenhard M, Jurgens G, Laux T. (1998) Role of WUSCHEL in regulating stem cell fate in the *Arabidopsis* shoot meristem. *Cell*. 95(6), 805-15.

BIBLIOGRAPHY

Mattsson J, Ckurshumova W, Berleth T. (2003) Auxin signaling in Arabidopsis leaf vascular development. *Plant Physiol.* 131(3), 1327-39.

McKeating JA, Zhang LQ, Logvinoff C, Flint M, Zhang J, Yu J, Butera D, Ho DD, Dustin LB, Rice CM, Balfe P. (2004) Diverse hepatitis C virus glycoproteins mediate viral infection in a CD81-dependent manner. *J Virol.* 78(16), 8496-505.

Miller BJ, Georges-Labouesse E, Primakoff P, Myles DG. (2000) Normal fertilization occurs with eggs lacking the integrin alpha6beta1 and is CD9-dependent. *J Cell Biol.* 149(6), 1289-96.

Mordhorst AP, Voerman KJ, Hartog MV, Meijer EA, van Went J, Koornneef M, de Vries SC. (1998) Somatic embryogenesis in Arabidopsis thaliana is facilitated by mutations in genes repressing meristematic cell divisions. *Genetics.* 149(2), 549-63.

Muller BM, Saedler H, Zachgo S. (2001) The MADS-box gene DEFH28 from Antirrhinum is involved in the regulation of floral meristem identity and fruit development. *Plant J.* 28(2), 169-79.

Mülhardt C. (2000) Der Experimentator: Molekularbiologie. 2. Auflage, Spektrum Akademischer Verlag GmbH, Heidelberg, Berlin.

Nadeau, JA, and Sack, FD. (2003). Stomatal development: Cross talk puts mouths in place. *Trends Plant Sci.* 8, 294-299.

Olmos E, Reiss B and Dekker K. (2003) The *ekeko* mutant demonstrates a role for tetraspanin-like protein in plant development. *Biochem. Biophys. Res. Commun.* 310, 1054-1061.

Ori N, Eshed Y, Chuck G, Bowman JL, Hake S. (2000) Mechanisms that control knox gene expression in the Arabidopsis shoot. *Development* 127(24), 5523-32.

Oren R, Takahashi S, Doss C, Levy R, Levy S. (1990) TAPA-1, the target of an antiproliferative antibody, defines a new family of transmembrane proteins. *Mol Cell Biol.* 10(8), 4007-15.

BIBLIOGRAPHY

Reinhardt D. (2003) Vascular patterning: more than just auxin? *Curr Biol.* 13(12), R485-7.

Reinhardt D, Pesce ER, Stieger P, Mandel T, Baltensperger K, Bennett M, Traas J, Friml J, Kuhlemeier C. (2003) Regulation of phyllotaxis by polar auxin transport. *Nature.* 426(6964), 255-60.

Reiser L, Sanchez-Baracaldo P, Hake S. (2000) Knots in the family tree: evolutionary relationships and functions of knox homeobox genes. *Plant Mol Biol.* 42(1), 151-66.

Rojo E, Sharma VK, Kovaleva V, Raikhel NV, Fletcher JC. (2002) CLV3 is localized to the extracellular space, where it activates the *Arabidopsis* CLAVATA stem cell signaling pathway. *The plant cell* 14, 969-977.

Sambrooke J, Fritsch EF, Maniatis T. (1989) Molecular cloning. *Cold Spring Harbor Laboratory Press.*

Sakamoto T, Kamiya N, Ueguchi-Tanaka M, Iwahori S, Matsuoka M. (2001) KNOX homeodomain protein directly suppresses the expression of a gibberellin biosynthetic gene in the tobacco shoot apical meristem. *Genes Dev.* 15(5):581-90.

Schoof H, Lenhard M, Haecker A, Mayer KFX, Jürgens G and Laux T. (2000) The stem cell population of *Arabidopsis* shoot meristems is maintained by a regulatory loop between the *CLAVATA* and *WUSCHEL* genes. *Cell* 100, 635-644.

Semiarti E, Ueno Y, Tsukaya H, Iwakawa H, Machida C and Machida Y. (2001) The *ASYMMETRIC LEAVES2* gene of *Arabidopsis thaliana* regulates formation of a symmetric lamina, establishment of venation and repression of meristem-related homeobox genes in leaves. *Development* 128, 1771-1783.

Serikawa KA, Martinez-Laborda A, Zambryski P. (1996) Three knotted1-like homeobox genes in *Arabidopsis*. *Plant Mol Biol* 32, 673-683.

BIBLIOGRAPHY

Smith LG, Jackson D, Hake S. (1995) The expression of *KNOTTED1* marks shoot meristem formation during maize embryogenesis. *Dev Genet.* 16, 334-348.

Smith HM, Boschke I, Hake S. (2002) Selective interaction of plant homeodomain proteins mediates high DNA-binding affinity. *Proc Natl Acad Sci U S A.* 99(14), 9579-84.

Ulmasov T, Murfett J, Hagen G, Guilfoyle TJ. (1997) Aux/IAA proteins repress expression of reporter genes containing natural and highly active synthetic auxin response elements. *Plant Cell.* (11), 1963-71.

Villanueva JM, Broadhvest J, Hauser BA, Meister RJ, Schneitz K, Gasser CS. (1999) INNER NO OUTER regulates abaxial- adaxial patterning in Arabidopsis ovules. *Genes Dev.* 3(23), 3160-9.

Williams RW. (1998) Plant homeobox genes: many functions stem from a common motif. *Bioessays,* 20, 280–282.

Weigel D, Alvarez J, Smyth DR, Yanofsky MF, Meyerowitz EM. (1992) LEAFY controls floral meristem identity in Arabidopsis. *Cell* 69(5), 843-59.

Yanai O, Shani E, Dolezal K, Tarkowski P, Sablowski R, Sandberg G, Samach A, Ori N. (2005) Arabidopsis KNOXI proteins activate cytokinin biosynthesis. *Curr Biol.* 15(17), 1566-71.

Xu H, Lee SJ, Suzuki E, Dugan KD, Stoddard A, Li HS, Chodosh LA, Montell C. (2004) A lysosomal tetraspanin associated with retinal degeneration identified via a genome-wide screen. *EMBO J.* 23(4), 811-22.

Zgurski JM, Sharma R, Bolokoski DA, Schultz EA. (2005) Asymmetric auxin response precedes asymmetric growth and differentiation of asymmetric leaf1 and asymmetric leaf2 Arabidopsis leaves. *Plant Cell.* 17(1), 77-91.

ERKLÄRUNG

Ich versichere, dass ich die von mir vorgelegte Dissertation selbständig angefertigt, die benutzten Quellen und Hilfsmittel vollständig angegeben und die Stellen der Arbeit – einschließlich der Tabellen, Karten und Abbildungen –, die anderen Werken im Wortlaut oder dem Sinn nach entnommen sind, in jedem Einzelfall als Entlehnung kenntlich gemacht habe: dass diese Dissertation noch keiner anderen Fakultät oder Universität zur Prüfung vorgelegen hat; dass sie – abgesehen von unten angegebenen Teilpublikationen – noch nicht veröffentlicht worden, sowie, dass ich eine solche Veröffentlichung vor Abschluss des Promotionsverfahrens nicht vornehmen werde. Die Bestimmungen dieser Promotionsordnung sind mir bekannt. Die von mir vorgelegte Dissertation ist von Prof. Wolfgang Werr betreut worden.

Wei-Hsin, Chiu

ACKNOWLEDGEMENTS

I would like to express the gratitude to my advisor professor Wolfgang Werr, for the continual guidance of my research and the substantial and detailed revising of the manuscript.

Also, I have to thank my colleagues in our lab. Annegret Flier, Britta Grewe and I not only help each other on work but also enjoy for several things together. Without their friendship, it is not easy to walk alone. And I should also thank other members of my lab for their help and information

I thank all my friends, in Germany and in Taiwan. Their encouragements and concerns during this work always keep me optimistic and active. Finally, my deepest gratitude goes to my mother. Without her support, I would never have the chance to study abroad.

LEBENS LAUF

Vor und Zuname	Wei-Hsin Chiu
Familienstand	ledig
Nationalität	taiwanesisch
Heimatadresse	83, San-De West St., San-Min Dist., 803, Kaohsiung, Taiwan.
Wohnanschrift	Clemens-August-Str., 76, App. 31, 53115, Bonn, Deutschland.
geboren am	18. 09.1976
geboren in	Hsinchu, Taiwan
1982-1994	Grundschule und weiterführende Schule
1994-1998	Studium mit Hauptfach Biologie National Cheng Kung Universität, Tainan, Taiwan
1998-2000	Studium auf der Hochschule im Institute of life science National Tsing Hua University, Hsinchu, Taiwan
2000-2001	Forschungspraktikum National Taiwan University, Taipei, Taiwan
2002-2003	Forschungspraktikum Institut für kognitive Neurologie, Tübingen
2003-2006	Doktorand Institut für Entwicklungsbiologie, Universität zu Köln